POWER LOSSES OF SILICON CARBIDE MOSFET IN HVDC

APPLICATION

by

Hsin-Ju Chen

B.S. in Electrical Engineering, University of Akron, 2010

Submitted to the Graduate Faculty of

Swanson School of Engineering in partial fulfillment

of the requirements for the degree of

Master of Science

University of Pittsburgh

2012

UNIVERSITY OF PITTSBURGH

SWANSON SCHOOL OF ENGINEERING

This thesis was presented

by

Hsin-Ju Chen

It was defended on

March 28, 2012

and approved by

William Stanchina, PhD, ECE Chairman and Professor, Department of Electrical and

Computer Engineering

Zhi-Hong Mao, PhD, Associate Professor, Department of Electrical and Computer

Engineering

Thesis Advisor: George Kusic, PhD, Associate Professor, Department of Electrical and

Computer Engineering

Gregory F. Reed, PhD, Associate Professor, Department of Electrical and Computer

Engineering

POWER LOSSES OF SILICON CARBIDE MOSFET IN HVDC APPLICATION

Hsin-Ju Chen, M.S.

University of Pittsburgh, 2012

Silicon carbide devices have advantages of higher blocking voltage, lower conduction loss, and lower low junction operating temperature compared to silicon-based devices. There's a need for more efficiency, economic and environmental friendly semiconductor devices for voltage source converter based high voltage direct current electric power transmission system application. This thesis compares a high power and high frequency operation of the SiC MOSFET with a conventional silicon IGBT module with similar power ratings in HVDC applications. An overview of the silicon carbide technology, power electronics and converter topology are also included. Two circuits were designed to compare the switching losses of SiC MOSFET with Si IGBT. The commercial SiC MOSFET QJD1210007 (1200V/100A) and Si IGBT CM100TF-24H (1200V/100A) were used in this study. PSCAD and Matlab/Simulink models of the devices were used to analyze the power losses. The models used in simulations are a preliminary evaluation of the device performance. The following studies were carried out: (i) A comparison between PSCAD and Matlab/Simulink simulation results for a push-pull converter, (ii) Switching power loss calculations via Matlab and accurate conduction loss estimation, (iii) and finally an experimental circuit was built to gather physical measurements to compare with the simulation results. The SiC MOSFET analytical was verified by comparing simulation with experimental switching waveforms. Based upon the experimental and analytical results, silicon carbide semiconductor devices have advantages over silicon IGBT and may replace them for HVDC applications. This thesis focuses on the simulation and physical circuit analysis.

TABLE OF CONTENTS

LIST OF TABLES

LIST OF FIGURES

x

ACKNOWLEDGEMENTS

1.0   INTRODUCTION

The applications of Si-based power transistors are limited due to low junction operating temperatures and low blocking voltage per devices. Megawatt power applications require efficient and high power-density converters that are capable of operating at elevated temperatures. With the improved performance of wide band-gap power semiconductors, such as like silicon carbide (SiC), gallium nitride (GaN) and diamond semiconductors, devices composed of such materials will improve converters [1-7]. SiC switching power devices have been developed throughout the last decade [8-9], to compliment SiC diodes already available in the market.

Cree, Inc., a semiconductor manufacturer, has developed new 1.2 kV; 100A Dual silicon carbide metal oxide semiconductor field-transistor (MOSFET) modules designed for high efficiency power conversion applications. Cree reported that when compared with a silicon insulated gate bipolar transistors (IGBT) module of equal rating device operating at a junction temperature of 150°C and 20 kHz, the SiC MOSFET module has 38% lower conduction loss and 60% lower switching loss. [10] The objective of this study was to compare the power losses of a commercial SiC MOSFET device to Silicon IGBT with a similar power rating. Experimental measurements were performed on a basic push-pull converter to verify the transistor power losses. Several software simulations were completed to predict the power loss of SiC MOSFET, and compare these results were later compared to those from experimental measurements. In

1

chapter 1, SiC technology is introduced; in chapter 2, semiconductor materials are introduced. The converter topology is presented in chapter 3; the hardware experiment and measurement are reported in chapter 4. Chapter 5 contains the conclusions and future work recommendations.

1.1 SILICON CARBIDE STRUCTURE

Power electronic applications in the field of power distribution and transmission systems have received attention because of their large-scale application. Market restructuring, environmental, and efficiency regulations in the world have led to innovations in power electronics for electrical power systems. Utility market restructuring and new regulations are aimed to improve the existing generation capacity, increase in efficiency, better use of existing plants, and provide environmentally acceptable ways of power transmission.

A variety of power semiconductor devices like diodes, thyristors, gate turn–off thyristors, metal-oxide semiconductor field–effect transistors, insulated bipolar gate bipolar transistors (IGBT), and metal-oxide semiconductor turn-off thyristors (MOSFET) are commonly used in the power electronics circuits. The need for improved performance of the electronic systems in high density applications has brought advancement in Si technology. However, Si devices are limited to operate at low junction temperatures and low blocking voltages. In megawatt power applications, which require more efficient, lightweight, high-density power converters operating at high temperatures, the development of wide band-gap semiconductors such as SiC, GaN, and diamond, are needed [1-11].

Silicon carbide has some unique properties, which make it a good material to overcome the limitations of silicon. [2-6] The wide band gap makes the device operate at high electric fields, and the reduction in intrinsic carrier concentration with increase in band gap enables the device to operate at high temperatures. SiC is a wide band gap semiconductor with high thermal conductivity, high breakdown electric field strength, high-saturated drift velocity, and high thermal stability. Therefore, silicon carbide is extremely durable and useful for many high power, high frequency, and high temperature applications. [1, 6-7]

However, Silicon Carbide devices have several defects that degrade their performance. Fabrication is one of the issues. The use of silicon carbide material is limited to small area devices and cannot extend to large size devices. The major manufacturing defects in silicon carbide devices are micropipes and screw dislocations. Nevertheless, SiC technology is an emerging technology and requires significant improvements to the material, device characterization, and modeling. Research in the material processing and fabrication technology, SiC has revolutionized the power electronics industry [5,6, 9-11]. Cree Co. demonstrated new SiC MOSFET devices at the APEC 2011 conference. The CMF20120D SiC MOSFET manufactured by Cree provides significant advantages over silicon devices, enabling unprecedented system efficiency and/or reduced system size, weight and cost through its higher frequency operation. [6, 9-10]

1.2   SILICON CARBIDE LATTICE STRUCTURE

SiC molecules are made by arrangement of covalently bonded tetrahedral Si and C atoms with either a carbon atom bonded to four Si atoms or a Si atom bonded to four carbon atoms as shown in Figure 1.1
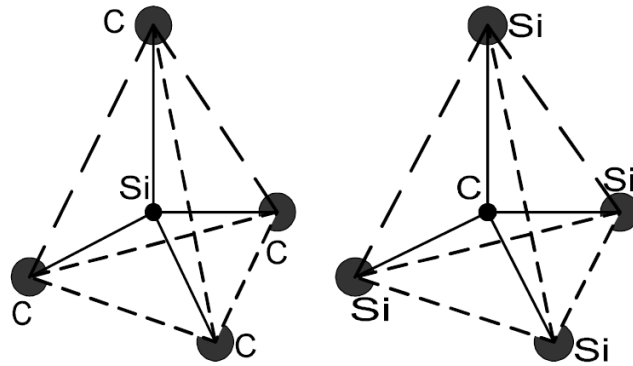
Figure 1.1 Tetrahedral silicon carbide structure [4]

SiC has many polytypes, which is made up of equal parts silicon and carbon. Both silicon and carbon are period IV elements, so they prefer a covalent bonding. Each carbon atom is surrounded by four silicon atoms, and vice versa. This leads to a highly ordered configuration, a single crystal, as shown in Figure 1.1. Silicon and GaAs have only one crystal structure; SiC has several structures.

The activation of parasitic structures of power MOSFET devices can be further divided into two categories: the activation of parasitic bipolar transistor (BJT) in power MOSFETs and the activation of parasitic diode in power MOSFETs. These failures can be triggered by different mechanisms when powers MOSFETs are used in a different harsh environment, such as extreme transient stress or a high radiation environment.

1.3 PROPERTIES OF SILICON CARBIDE

The typical properties of various semiconductors are listed in Table 1-1.The advantage properties of SiC compared with other semiconductor devices as mentioned in Section 1.1 are discussed in more detail in the following:

Table 1-1 Semiconductor properties[1-7]

	Si	4H-SiC	6H-SiC	GaAs	GaN	Diamond
Energy bandgap, E_g (eV)	1.12	3.03	3.26	1.43	3.45	5.45
Critical electric field, E_c (MV/cm)	0.25	2.2	2.5	0.4	2	10
Saturated electron drift velocity, v_{sat} (cm/s)	1×10^7	2×10^7	2×10^7	1×10^7	2.2×10^7	2.7×10^7
Thermal conductivity, l (W/cm-K)	1.5	4.9	4.9	0.46	1.3	22
Electron mobility μ_n (cm2 /s)	1350	1000	500	8500	1250	2200
Dielectric constant e_τ	11.9	10.1	9.66	13.1	9	5.5

1.3.1 Wide Bandgap

Silicon carbide is classified as a wide band gap material ($E_g = E_c - E_v$), where E_c is conduction band energy, E_v is valence band energy, and E_g is band gap. The high velocity saturation and thinner drift region associated with the high band gap make the device operate in higher

frequency environment. Due to high band gap, silicon carbide has reduced drift region width, and hence less conduction [6-7]. Therefore, the on-resistance of silicon carbide devices is lower and results in lower conduction losses compared to other devices. Figure 1.2 shows the specific on-resistance vs. the designed breakdown voltage of Si, and 4H and 6H SiC. GaAs is 12-fold better than Si; GaN is two-fold better than SiC. The breakdown voltage is the voltage at which the reverse-biased body-drift diode breaks down and significant current starts to flow between the source and drain by a valance multiplication process, while the gate and source are shorted. For most power devices the current is conducted through the substrate. This adds some resistance since the mobility and the amount of doping is limited. Wider energy band gap also supports in much lower leakage currents and slightly provides higher operating temperatures. Radiation hardness is also improved. [2]
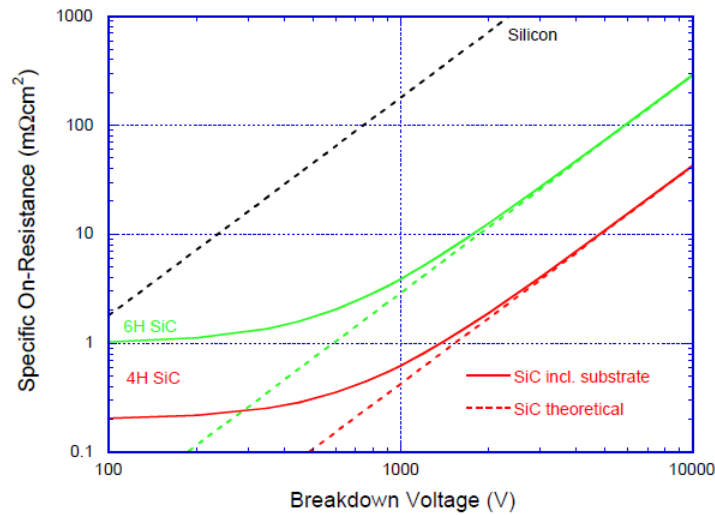
Figure 1.2 Specific on-resistance vs. the designed breakdown voltage of silicon carbide [4]

6

1.3.2   Critical Electric Field
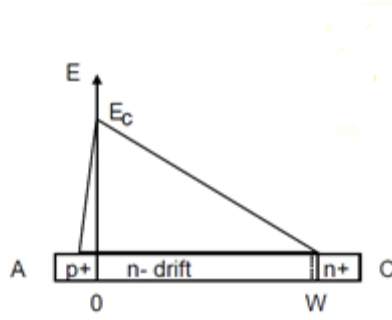
Figure 1.3 The electric field of a semiconductor [4]

The idea with a semiconductor device is that they can either block a voltage, or conduct a current with low power loss. As seen in Figure 1.3 that the W is depletion region width at the electric field distribution inside the device. Most of the depletion region spreads into the lowest doped part of the junction. [8]

$$V_B = \frac{W\, E_c}{2} \tag{1}$$

$$W \approx \sqrt{\frac{2\, \varepsilon V_B}{q\, N_D}} \tag{2}$$

$$N_D = \frac{2\varepsilon V_B}{q\, W^2} = \frac{\varepsilon\, E_c^{\,2}}{2qV_B} \tag{3}$$

$$R_{on,sp} = \frac{W}{q\, \mu_N N_D} = \frac{4\, V_B^{\,2}}{\varepsilon\, \mu_N E_c^{\,3}} \tag{4}$$

$$\frac{V_B^{\,2}}{R_{on,sp}} = \frac{\varepsilon\, \mu_N E_c^{\,3}}{4} \tag{5}$$

From equation (1), the voltage supported by this depletion region can be calculated, which is the area under the graph. The lower critical electric field makes the lower on resistance and lower

7

switching losses as calculated from equation (2) to (4).When the device is not blocked, it will conduct large currents with small voltage drop (power loss). Equitation (5) shows that the higher electric field leads to higher doping which is the lower on-resistance in the devices. The minority carrier charge has to be removed before the device can block a voltage, and this will result in a switching loss [13]. The total loss is on-state loss plus switching frequency times switching loss. Higher critical electric field means that blocking layers of the devices can be thinner and with higher doping concentrations, contributes to lower on- resistance values compared to the equivalent silicon devices [6].
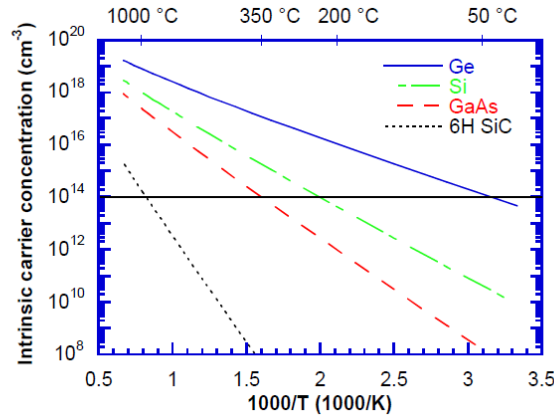
Figure 1.4 Intrinsic concentration v.s. temperature with various material semiconductors [22]

1.3.3 High saturated drift electric field

The electron and hole mobility shows how an electron/hole can move through a semiconductor. In a solid, electrons/holes move around randomly without any applied electric field. At low fields, the drift velocity is proportional to the electric field, so mobility μ is constant. [3,7] Therefore, due to the high electric field, the drift regions of SiC are thinner, and hence lead to

higher operating frequencies. Moreover, the reverse recovery current passing through the wide bandgap semiconductor will be smaller, and hence the recovery time will be shorter.

1.3.4   High thermal conductivity

Thermal conductivity is the property that gives a material the ability to conduct heat transfer. Higher thermal conductivity (e.g., SiC and diamond) improves heat spreading and allows operation at higher power densities. [13] With respect to the higher thermal conductivity and low coefficient of thermal expansion (4.0×10^{-6}/K), SiC has better heat dissipation than Si, and thus requires less heat sink. Due to the low intrinsic carrier concentration and wider band gap, SiC has an intrinsic temperature of 900°C while Si has 200°C. High thermal conductivity enables SiC devices to operate at extremely high power levels and still dissipate the large amount of excess heat. Therefore, the cost of cooling accessories like heat sink will be much less than silicon devices.

1.3.5   High Electric Breakdown Field

SiC has a higher breakdown field than silicon because of the wide band-gap. The electron-hole pair generation due to ionization impact is difficult because of the wide band gap, and hence SiC can withstand higher electric fields compared to silicon. The high electric breakdown field allows the device to have less thick layers compared to silicon and therefore less drift region resistance reducing the on-state losses. [12]

1.3.6 Summary of the advantages of SiC

In summary, SiC has the following advantages over Si:

- Wide band gap => reduce carrier concentration => high temperature
- Wide band gap => better dynamic response
- High critical field => reduce drift region widths=> low on-resistance
- High electric field => block higher voltage
- High velocity saturation and Low   permittivity => faster switch, high frequency
- Smaller size and weight
- High thermal conductivity => high power and better heat dissipation
- Bipolar => lower recovery current => less switching loss

The most important advantage of SiC is the high critical field for breakdown voltage, which is good for all devices. Wide band gap materials exhibit greater electron mobility with larger applied fields compared to Si. Intrinsic parameters translate to enhanced operation at high switching frequencies with high breakdown voltage. Gallium nitride, in some respects, is a better material than SiC. The big difference is the energy band gap. Silicon has an almost three times smaller band gap than the wide band gap materials SiC and GaN. However, there is about a ten times wider critical electric field for breakdown that makes the huge difference. There are no large differences in the other parameters, except the high mobility of GaAs. [32-36] Diamond is overall the best material for high power, high current density, lower conduction loss, fast switching, and high-temperature operation. However, diamond is not expected to be abundant, due to the higher material and processing cost. The other advantage of SiC is that the cost of SiC devices is much lower than that of GaN, GaAs, or diamond.

Since the gate structure of power MOSFETs are similar to that of lateral MOSFETs, only the inherent parasitic structures of power MOSFET are addressed here. The inherent parasitic structures in power MOSFET include a parasitic bipolar transistor and a parasitic diode.

1.4 DYNAMIC CHARACTIEISTICS

When the MOSFET is used as a switch, its basic function is to control the drain current by the gate voltage. The switching performance of a device is determined by the time required to establish voltage changes across capacitances.

The equivalent circuit, as shown in Figure 1.5, is used for analyzing the power losses dissipated from the transistor by varying the voltage, current, or capacitance. This circuit is widely used in all power electronics topologies including DC-DC converters and inverters for estimating the power MOSFET drain-to-source switching loss. The three inter-electrode parasitic capacitances of the power transistor provide the simplified switching waveforms for estimating the switching power losses.
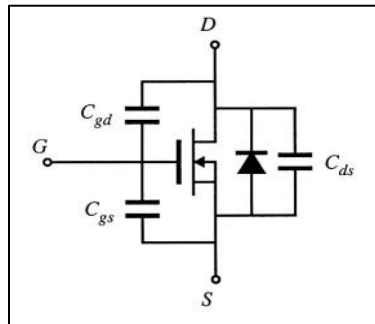
Figure 1.5 Typical switching time test circuit [18]

The method of estimating power MOSFET intrinsic capacitances of C_{GD}(gate-to-drain capacitance), C_{GS}(gate-to-source capacitance), and C_{DS} (drain-to-source capacitance) are based

on equation (6)-(8) where C_{ISS} is the input capacitance with drain and source terminal shorted; C_{RSS} is reverse transfer capacitance with gate and source terminal shorted; C_{OSS} is output capacitance with gate and source terminal shorted. Manufacturers prefer to quote C_{ISS}, C_{OSS}, and C_{RSS} because they can be directly measured on the transistor. However, the parasitic capacitance C_{GS}, C_{GD}, and C_{DS} are closer to the physical meaning. Although input capacitance values are useful, they do not provide accurate results when comparing the switching performances of two devices from different manufacturers [15-19].

$$C_{GD} = C_{RSS} \qquad\qquad (6)$$
$$C_{GS} = C_{ISS} - C_{RSS} \qquad\qquad (7)$$
$$C_{DS} = C_{OSS} - C_{RSS} \qquad\qquad (8)$$

The advantage of using gate charge is that the designer can easily calculate the amount of current required from the drive circuit to switch the device on in a desired length of time; since Q = CV and I = C dV/dt then Q = time x current. The input capacitance parameters were not reflect to these equations.
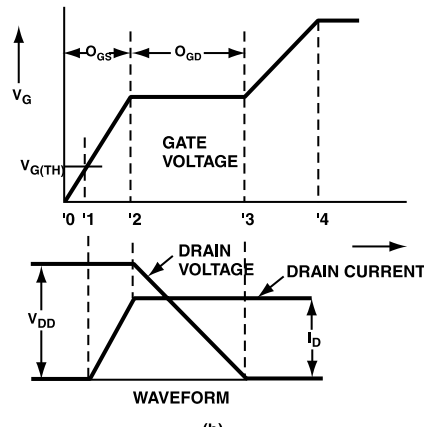
Figure 1.6 Resulting gate and drain waveforms [15-18]

The University of Central Florida reported how the transit capacitors affect the transistor power losses. The gate charge switching test circuit is shown in Figure 1.5, where the research

12

team put the device and its model components into a drive circuit with an inductor and freewheeling diode. It can be used to analyze the power losses dissipated from the transistor by varying the voltage, current, or capacitance. [17-18]

In this study, the switching circuit was plugged into a boost converter in PSCAD. The purpose was to evaluate the power losses from different semiconductor materials. The following circuit was used to compare the power losses of the transistors with different materials where the external capacitances were added into the transistors.
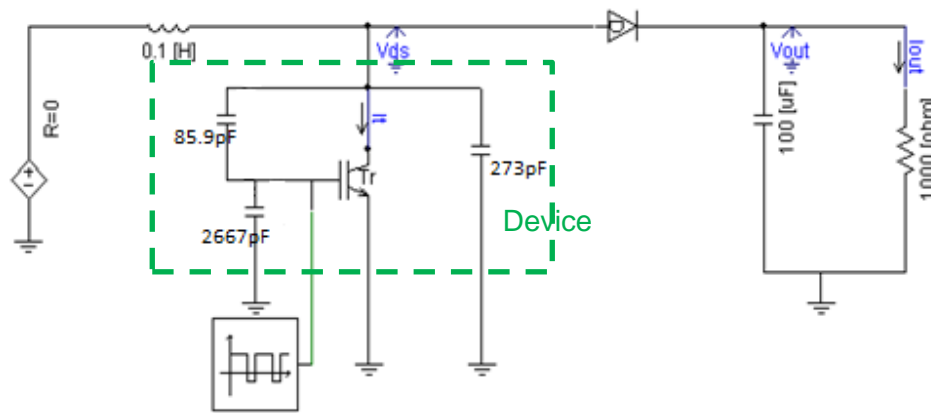
Figure 1.7 Boost converter with testing circuit via PSCAD

Table 1-2 lists the intrinsic capacitance of the devices where the GaN device was taken from Reference [3]; the Si and SiC device intrinsic is calculating by equation (1) to (3) as mentioned in the previous section. The parameters were used in the boost converter with a testing circuit and simulated via PSCAD.

Table 1-2 Intrinsic capacitance data of GaN, Si, and SiC [3,20,21]

Material	Model	C_{GD} [pF]	C_{GS} [pF]	C_{DS} [pF]
GaN	Virtual HEMT	85.9	2667	273
Si	Qjd1210007	133	10100	900
Sic	CM100TF-24H	4000	16000	3000

The power dissipated by the different transistors and loads should very since the characteristics will result in different turn-on and turn-off behavior. However, the results from PSCAD and Simulink had the same waveforms and values between the three materials at the same voltage rating as shown in Figure 1.8.
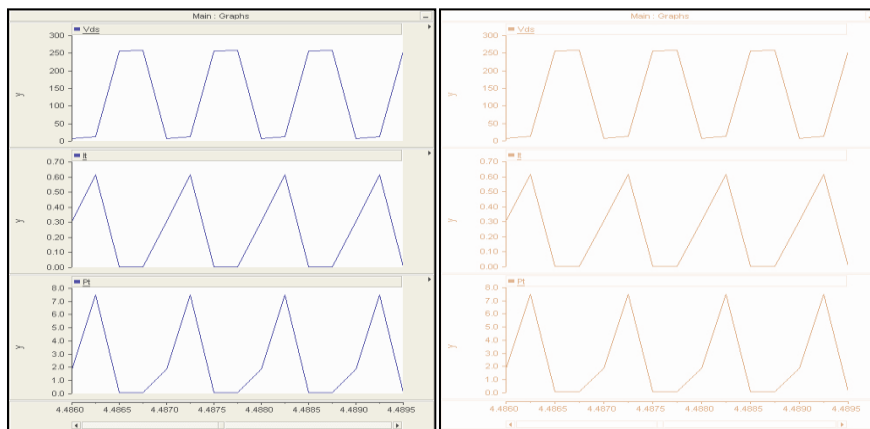
Figure 1.8 Intrinsic capacitance experiment via PSCAD result

The reason it showed the same results is that the capacitors had negligible effect on losses compared to the other elements in the circuit. PSCAD simulates the circuit by taking from each node. In addition, the transistors appear as a pure resistance in the circuit.

1.5   FAILURE MECHANISM OF POWER DEVICES

In this section, the failure mechanisms of Schottky diodes, power MOSFETs, and IGBT are reviewed respectively.

Since the gate structure of power MOSFETs are similar to that of lateral MOSFETs, only the inherent parasitic structures of power MOSFET are introduced here. The inherent parasitic structures in power MOSFET include a parasitic bipolar transistor and a parasitic diode[61-66]. The

advantage of the Schottky diode is that it can operate in a high switching frequency environment with low forward voltage drops. Also, it can be placed parallel to any type of semiconductor device to cause the on-state currents of the devices to be equal. [22-24]

1.6   SILICON CARBIDE POWER DEVICES

The development of power semiconductor devices has always been a driving force for power electronics systems. Silicon based power electronic semiconductor devices have been widely used for high voltage, high frequency application. Due to the physical properties, silicon semiconductors are not able to operate at high-power frequency, and resulting in lower efficiency. As discussed in Sections 1.1 and 1.3, silicon carbide IGBT can operate at high voltage over 5 kV and high current over 1000 A, whereas the bipolar nature of the device limits the switching frequency of converter systems below 100 kHz; thus, the efficiency and integration of the system were improved. [6] The main advantage of the SiC Schottky diode is the lack of reverse voltage recovery charge across the diode.

Furthermore, the general 150 ^{o}C limit of maximum junction temperature also hinders the use of Si devices in high-power-density and high-temperature situations.[20] This increases the blocking capability of SiC power devices and also allows them to be fabricated with much thinner and higher doped drift layers, significantly reducing the on-state resistance. The high thermal conductivity of SiC (4.9 W/cm-K) enhances heat dissipation and, coupled with the wide band gap energy (3.3 eV), allows high-temperature operation above 300 °C. All of the above advantages make the SiC power devices an ideal substitution for Si counterparts in high-voltage and high-power converter systems. [20-21]

Compared to conventional devices with the same voltage rating, these SiC active switches provide much lower on-state resistance than Si MOSFET and much higher switching speed than Si IGBT. This is promising for resolving the trade-off between high frequency and high efficiency for 600-800 V energy conversion systems. [1, 22]
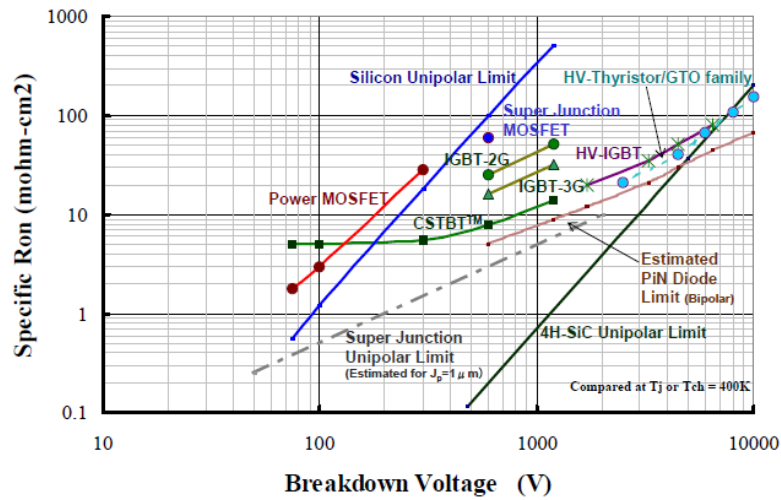
Figure 1.9 Relationship on specific-on-resistance and breakdown voltage[30]

1.7   DEVICE SELECTION

Power losses of silicon carbide power MOSFET devices are next compared to transistors of other material systems.   Commercial SiC MOSFET QJD1210007 (1200V/100A) and Si IGBT CM100TF-24H (1200V/100A) were selected in this study. The SiC device was designed for high power applications. The packaging of the devices includes with two MOSFET transistors in half-bridge configuration with each transistor reversely connected with a free-wheel silicon carbide Schottky diode.

16

Cree, Inc. has introduced a new 1,200V, 100A dual SiC MOSFET module for power conversion applications. They reported that when compared to a silicon IGBT module with an equal rating device to operate at a junction temperature of 150°C and 20kHz, the SiC MOSFET module has 38% lower conduction loss and 60% lower switching loss.[2] However, there are significant power losses in SiC MOSFET devices operating at high voltage. The objective of this study was to compare the power losses of the commercial SiC MOSFET device to the conventional Si IGBT module with a similar power rating. The commercial SiC MOSFET QJD1210007 (1200V/100A) from POWEREX Inc. and Si IGBT CM100TF-24H (1200V/100A) from Mitsubishi Electric were selected in this study.

1.8   RESEARCH MOTIVATIONS AND OBJECTIVES

With great progress in the improvement of SiC active switches, much effort has been invested in studying the SiC IGBT and MOSFET characteristics and their potential utilization in power converter systems. Temperature-dependent characteristics of the two devices have been extensively studied. Different physics-based and behavior device models have also been developed for SiC IGBT and MOSFET. [6, 14]

This thesis focuses on the power losses of Si IGBT and SiC MOSFET for HVDC applications. The purpose of this work is to support the development of a high-frequency isolated DC-AC-DC converters aiming at reducing the passive component sizes and boosting system power density. To achieve this goal, Si IGBT from Mitsubishi Electric and SiC MOSFET from Powerex, both with 1.2 kV voltage rating, were characterized in this study. Issues regarding the model accuracy are discussed, and the solutions are provided as well. In this study, a generalized

17

model using MATLAB/SIMULINK was developed to obtain the power losses of SiC MOSFET and IGBT.

The IGBT technology is the device for higher power and lower frequency, while MOSFET is for lower breakdown voltage but higher frequency. However, choosing between IGBTs and MOSFETs is very application specific. The cost, size, speed and thermal requirements are also important.

2.0   POWER SEMICONDUCTORS TOPOLOGIES

Semiconductor power devices act as a switch for high power applications. Power semiconductor devices are functional elements in all power conversion applications specific in high power and high frequencies. As a result, the devices are used as switches to convert power from one form to another. Different switches have different performance based on the power process being performed. This chapter will briefly introduce power electronic devices for high-power and high-frequency applications and will also provide the power electronic circuits developed with Matlab/Simulink packages.

2.1   PERFORMANCE CHARACTERISTICS

This section will briefly introduce the switch function. In addition, the Matlab/Simulink simulation results will be presented.

2.1.1   Ideal Switch

The ideal switch is a physical device that simplifies semiconductor devices by means of current chopping. The switch is fully controlled by the gate signal as show in Figure 2.1. When the switch is open, the switch blocks any forward voltage with no current flow; when the switch is

closed, the switch conducts all bidirectional currents with quasi-zero voltage drop. Therefore, there will be no losses dissipated through an ideal switch.
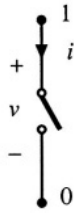
Figure 2.1 Ideal switch symbol [17]

Figure 2.2 illustrates the diode symbol which contains two power terminals: 1 and 0. In the on state, the voltage is zero, while the current is zero in the off state. The diode can block negative voltage but not positive voltage.
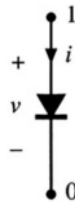
Figure 2.2 Diode Symbol

The following circuit (Figure 2.3) uses the ideal switch to switch an RLC load with a 120Vrms, 60Hz AC power supply [23] simulated with Matlab/Simulink. The switch is initially closed and will be turned off after 3 cycles, then reclose at 8.25 cycles.
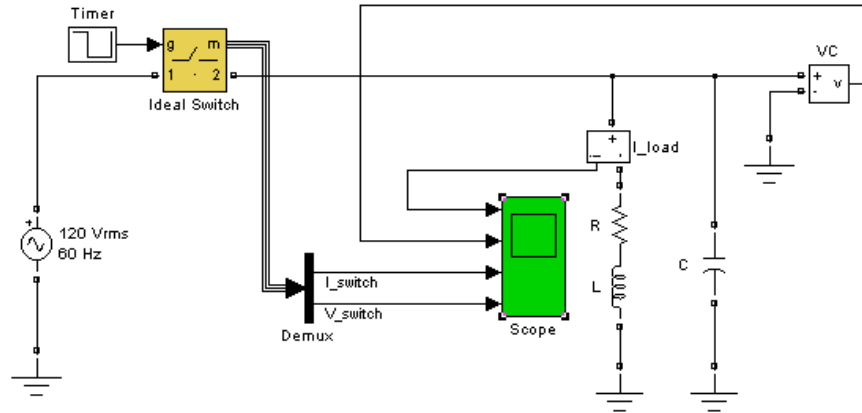
Figure 2.3 Ideal switch in switching circuit via Matlab/Simulink [23]

Figure 2.4 shows the simulation result observed by Simulink from Figure 2.3 circuit. The results show that the inductor current chopping produced the high frequency overvoltage. When the switch reclosed, the capacitor reached maximum source voltage and created the highest switch current spike.
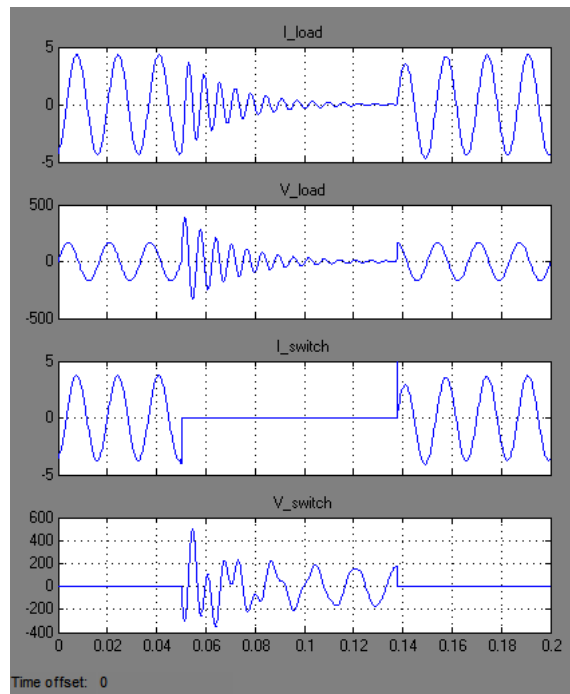
Figure 2.4 The voltage and current waveforms of the RLC load and switch observe from the ideal switch circuit via Matlab/Simulink

21

2.1.2   Metal Oxide Semiconductor Field-Transistor (MOSFET)

Power MOSFETs are essentially voltage-driven devices. The basic principle of a MOSFET device is that the voltage on the oxide-insulated gate electrode can induce a conducting channel between source and drain. The MOSFET conduct the peak current to exceed its average current. It is a voltage-controlled device with gate current flow during operation.
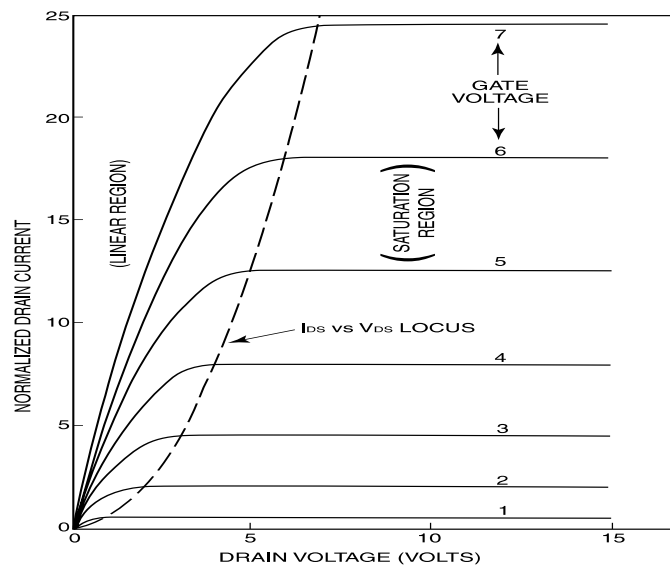
Figure 2.5 Current-voltage characteristics of a power MOSFET [17]

Figure 2.5 shows I–V characteristics of an enhancement mode power MOSFET. [17] This graph is used to determine if the device is in the full on-state or in the constant-current region for a given value of gate and drain current. Figure 2.6 illustrates a MOSFET equivalent circuit where the gate drive circuit is supplying the MOSFET to raise the gate voltage with a specified value of off state drain-to-source voltage. The gate charge is the total charge on the gate-to-drain and the gate-to-source capacitance supplied by the gate drive circuit. The drain current change is dependent on the rate at which the gate-to-source capacitance is charged by the gate drive circuit.

22

The drain-to-source capacitance leads directly to switching loss in PWM converters, since the energy stored in this capacitance is lost during the transistor turn-on transition. In general, there is a body diode inherent with the power MOSFET devices. It enables the MOSFET to conduct in full rated current. However, the body diode operates at a slower switching frequency than the MOSFET and might cause device failure.
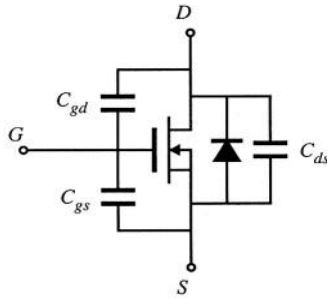
Figure 2.6 MOSFET equivalent circuit [17-18]

The same circuit (Figure 2.3) was used to measure the behavior of MOSFET. The observed waveforms are shown in Figure 2.7, illustrating that the positive current was block out by MOSFET devices during the switch on state. As seen in the switch voltage and current plots, the MOSFET can block positive voltage and will be able to carry a positive or negative current [78].
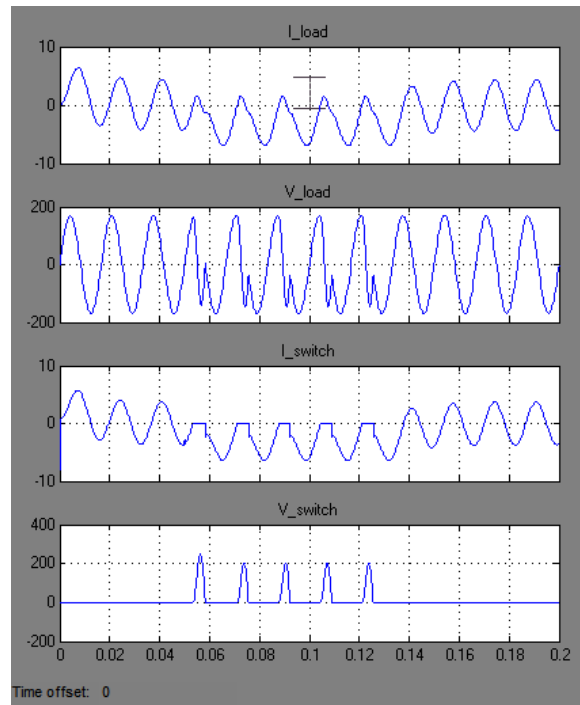
Figure 2.7 MOSFET characteristic simulation result from switching test circuit

2.1.3 Insulated Gate Bipolar Transistor (IGBT)

The insulated gate bipolar transistor (IGBT) is a three-terminal power semiconductor device. The IGBT devices were developed with small gate power consumption to turn on and off rapidly and often used to generate complex waveforms with pulse width modulation. These devices are used in many HVDC applications due to high efficiency, fast switching, low conduction voltage drop, and high current carrying capability. [15-17]

24
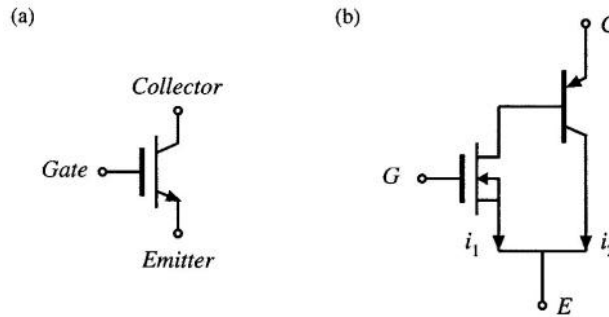
Figure 2.8 IGBT symbol [17]

The IGBT combines the simple gate drive characteristics of the MOSFETs with the high operation current and blocking voltage by combining an isolated gate FET for the control input and a bipolar power transistor as a switch. The IGBT has bi-directional current carrying capabilities. Thermally assisted carrier multiplication is proposed as the failure mechanism of IGBTs. [17] Current flow through a high electric field region leads to significant power dissipation, which makes the devices self-heating. By increasing the switching frequencies to the low kHz range of pulse width modulation to the gate, one can control the output magnitude and harmonic distortion. Typical IGBT applications include operating at low duty cycle, low frequency (<20kHz), high junction temperature (>100°C), and high-voltage applications (>1kV).

The same circuit (Figure 2.3) was used to perform the behavior of IGBT. The observed waveforms are shown and illustrate that negative current and voltage were blocked out by IGBT devices during the switch on-state.
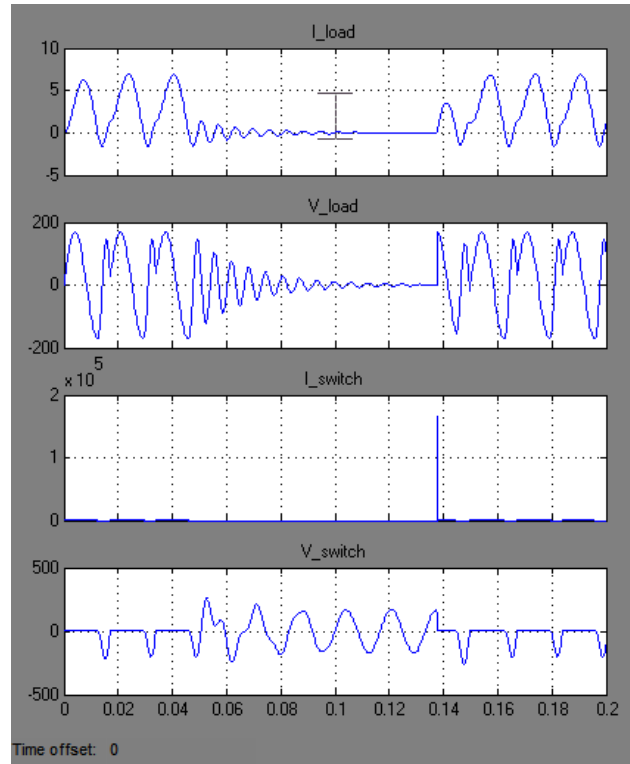
Figure 2.9 IGBT characteristic observed via Simulink

2.2   COMPARISON OF IGBT AND MOSFET DEVICES

IGBT and power MOSFET devices are very similar in construction. The key difference is the *p* region connected to the collector of the IGBT. Therefore, the IGBT is a modern four-layer power semiconductor device having a MOS gate. The on-state voltage across the IGBT is one diode voltage drop higher than for the N-channel power MOSFET by itself. However, compared to a conventional high voltage power MOSFET of the same size and similar power rating, the IGBT has significantly lower on- state voltage. IGBT is the device of choice for high current and high voltage application because of the easily driven MOS gate and low conduction loss. [24] The tradeoffs with lifetime control are an increase in on-state voltage called V_{C-E} and slightly higher

26

leakage current at high temperature. Increase on-resistance with increasing breakdown voltage ratings, and power MOSFETs rated at or above about 300 Volts have lower current densities than IGBTs.

Turn-on characteristics of an IGBT are very similar to a power MOSFET. Turn-off differs because of the tail current. Thus, the turn-off switching energy in a hard switched clamped inductive circuit gives an indication of the switching speed and tail current characteristic of an IGBT. Figure 2.10 depicts the tradeoff between turn-off switching energy E_{off} and $V_{CE(on)}$. At high frequency and relatively low currents, a MOSFET is usually the best choice. (V-I characteristic, breakdown characteristic, turn-on, and turn-off characteristics were not discussed here.)
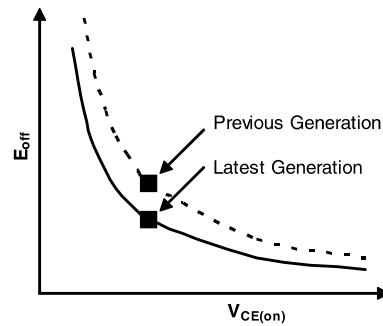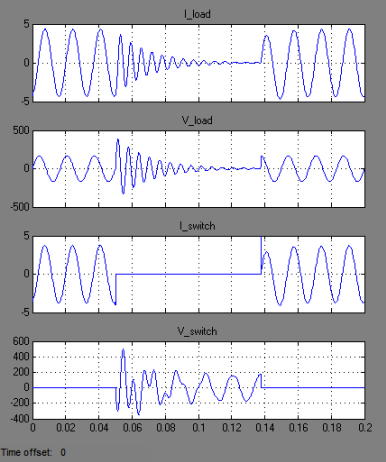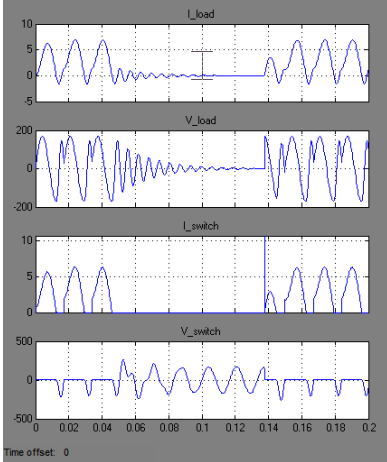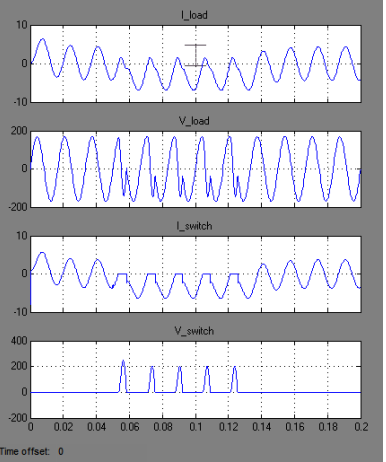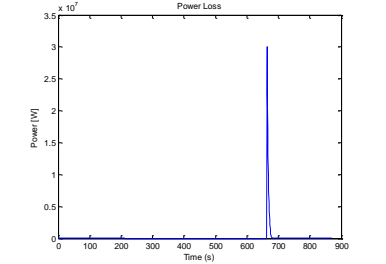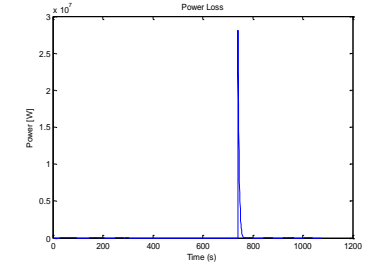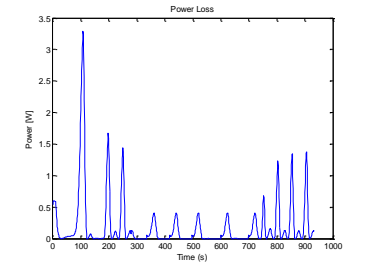
Figure 2.10 Turn-off voltage versus V_{CE}[24]

2.2.1   Simulation comparison results

Table 2-1 presents the simulation results from Figure 2.3 circuit. As discussed in the last section, there is no parallel diode to the IGBT, so there is no negative current passing through the IGBT switch as shown in Table 2-1 Switching circuit simulation results with different type of switches via Matlab/Simulink switch current plots. The on-resistance of the MOSFET is as well as the forward voltages are higher. As shown in the switching voltage plots, the ideal switch has

27

highest switching voltage, IGBT has the second, and MOSFET has the least. The table also

shows that the MOSFET has the smallest power loss while the ideal switch and the IGBT have

about the same loss.

Table 2-1 Switching circuit simulation results with different type of switches via
Matlab/Simulink

Ideal Switch	IGBT	MOSFET

28

2.3   TRANSISTOR POWER LOSSES

During a switching transition, very large instantaneous power loss can occur in the semiconductor devices. Even though the semiconductor switching times are short, the resulting average power loss can be significant. [25]

Power loss is critical for highly integrated power MOSFETS since they dissipate much more power than any other device. Power dissipation in the power semiconductors is primarily dependent on their on-resistance, gate charge factors, current, voltage rise and fall times, and the switching frequency and operating temperature

The power loss in any semiconductor is caused by the combination of the switching losses, conduction losses, blocking (leakage) losses, body diode conduction loss, and gate drive loss. [14, 26] Normally the leakage losses and other losses are being neglected as demonstrated in equation (9). The switching loss is when the losses occur during the switch turn-on and turn-off periods, while the conduction loss occurs during the switch conducts.

$$P_{MOSFET} = P_{Switching} + P_{Conduction} + P_{Leakage}$$
$$\cong P_{Switching} + P_{Conduction}$$

(9)

This thesis focused on the transistor loss. Other losses from the converter were neglected because they are too small.

2.3.1   Conduction Loss

The conduction loss is the loss from an on-resistance of the transistor that is generated when the drain current goes through the body diode during dead time. An on-resistance is the intrinsic resistance from drain-to-source of a semiconductor device, usually represented as $R_{DS,ON}$ or R_{ON}

[69, 70]. When the gate drive signal is high, the transistor turns on, and conducts the current and power dissipated through the device. There are many factors which may effect on-resistance, such as temperature and input voltage. The on-resistance of a transistor is temperature-dependent: higher temperature provides higher on-resistance. [14, 17] Therefore, the data sheet of a power MOSFET module usually has the data record or an on-resistance versus temperature plot. Figure 2.11 is the on-resistance plot normalized with temperature from data sheet of QJD1210007. On-resistance R_{on} can be verified from I-V characteristics by taking the derivative with respect to current I_F and rearranging items in equation (10):

$$R_{on} = \partial(V_F - n_{kT}) * \partial I_F * q * I_F \tag{10}$$

NORMALIZED ON-RESISTANCE
VS. TEMPERATURE
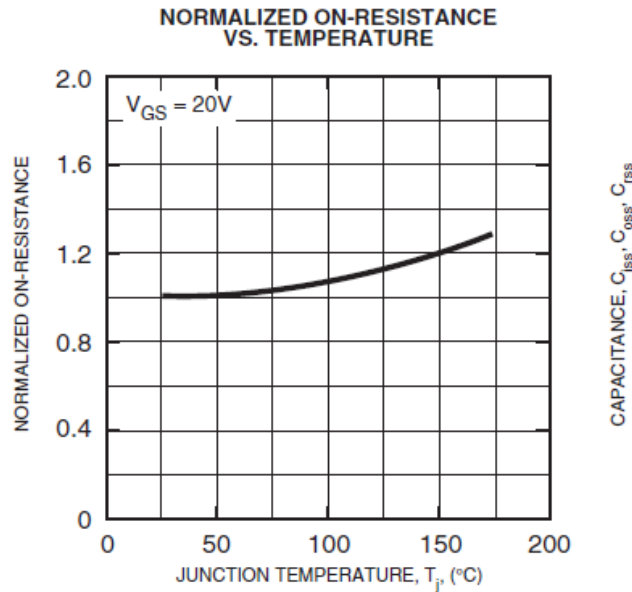
Figure 2.11 QJD1210007 on-resistance versus junction temperature [76]

While the transistor is turning on or off, its intrinsic parasitic capacitance stores or dissipates energy during each switching transition. The losses are proportional to the switching

30

frequency and the values of the parasitic capacitances. As the capacitance increases, the switching power losses also increase. When the full input voltage swings, the full current will pass through it, which causes the brunt of the switching losses. In order to get the average value of the conduction loss, simply multiply the above expression as represented in Eq. (11) by the duty ratio of the MOSFET. [1, 14-17]

$$P_{conduction} = I_{on}^2 * R_{DS(ON)} \qquad (11)$$

Notice that, I_{on} is the drain current when the MOSFET is on, and $R_{DS(ON)}$ is the drain-source resistance of the MOSFET when it is on. To get the average value of the conduction loss, one can simply multiply the above expression by the duty ratio of the MOSFET.

If the transistor is an ideal switch, there would be no conduction power loss. In order to reduce the conduction loss, on-resistance must be minimized, which requires more silicon and results in a cost increase. Hence, there is a trade-off between the conduction loss and silicon cost.

2.3.2   Switching loss [6, 15-18]

Switching losses are due to the nonzero product of the drain current and drain to source voltage. As the MOSFET switches on and off, its intrinsic parasitic capacitance stores and then dissipates energy during each switching transition. The losses are proportional to the switching frequency and the values of the parasitic capacitances [17, 19, and 26]. As the physical size of the MOSFET increases, its capacitance also increases. In other words, increasing MOSFET size will increase switching loss. [6] If the MOSFET is an ideal switch, the device rise and fall times of the current and voltage would be zero, and there would be no switching loss. [16-18]

$$P_{sw1} = \frac{t_{sw,on} * V_{off} * I_{on} * f_{sw}}{2} + \frac{t_{sw,off} * V_{off} * I_{on} * f_{sw}}{2} \qquad (12)$$

Notice that, V_{off} is the drain source voltage when the MOSFET is off

$t_{sw,on}$/ $t_{sw,off}$ is the time it takes to turn the MOSFET on / off

f_{sw} is the switching frequency

Another form of switching loss is the drain-source parasitic capacitance of the MOSFET charging/discharging as shown in equation (13). [19] Comparing to the input capacitance and reverse transfer capacitance, the output capacitance has more effect on the switching loss.

$$P_{sw2} = C_{OSS} * V_{off}^2 * f_{sw} \tag{13}$$

where C_{OSS} is the output capacitance of the MOSFET. The way to observe C_{OSS} were discussed in Chapter 1.

The energy W_{off} dissipated during the switching turn-off period is the area under the curve of both voltage and current waveforms as shown in Figure 2.12. Therefore, during one switching period, the total switching losses dissipated by a transistor is the combination of the turn-on energy (W_{on}) and turn-off energy (W_{off}) proportional to the frequency. From both equations (12) and (13), it is shown that the switching loss is proportional to the switching frequency, turn-on, and turn-off switching times. In power electronics, the switching losses typically contribute a significant amount to the total system losses. To minimize the switching loss, reducing the switching frequency will result in increasing the inductance and size for a given inductor ripple current. Also, turning-on and off the MOSFETs faster is another way to minimize the switching loss.
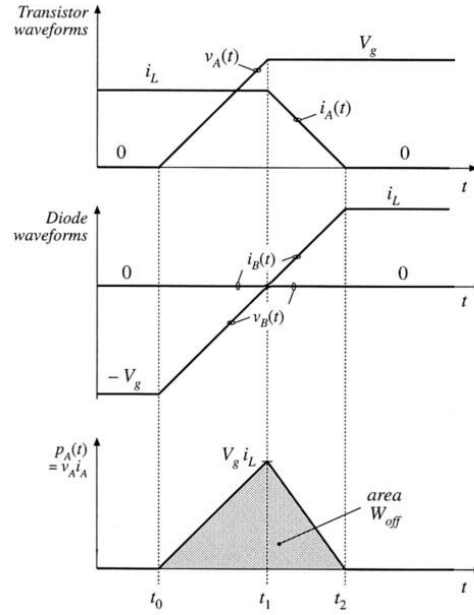
Figure 2.12 Switching power losses waveform [17]

As shown in Figure 2.13, the drain-to-source voltage (blue line) and drain current (red line) of the power MOSFET are plotted. For an ideal switch case, when the voltage turns on, the current turns off, and vice versa. Since there is no delay time between switch on and off, there is no switching loss. For the conduction loss, when the voltage turns on, the current turns off, meaning that, there is no current flow. Therefore, there is no conduction loss during this time. The same situation occurs when the current runs on: the voltage will be zero, and the conduction loss is zero. Finally, in an ideal switch case, there is no power loss dissipated by the transistor.

Figure 2.13 illustrates a non-ideal switch. The conduction loss is the hexagon (shown in orange area) area. Similar to the ideal switching case, when the voltage or current is zero, there is no conduction loss during that period. This implies that the conduction is only the two triangles on the left and right of the hexagon. In reality, the current is not zero, and as is the voltage, so the conduction loss is the hexagon (blue) area. The switching loss is the area underneath of the switching period, as seen in the green triangle area from the plot.

33
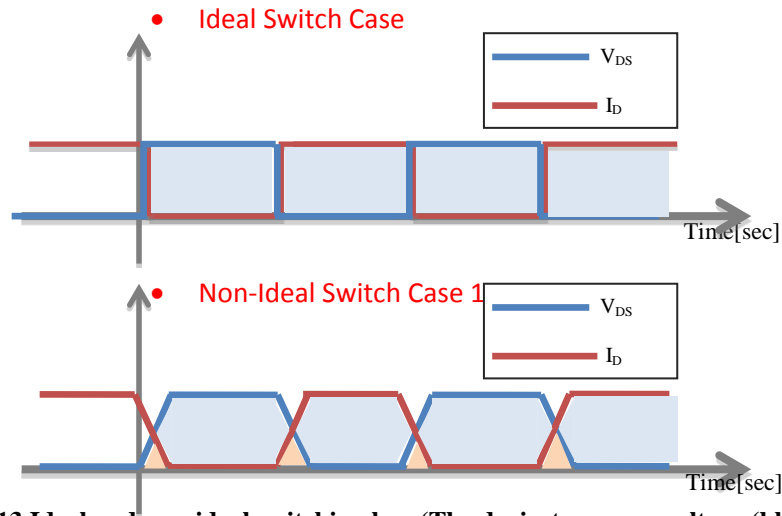
Figure 2.13 Ideal and non-ideal switching loss (The drain-to-source voltage (blue line) and drain current (red line) of the power MOSFET

In general, when the switching frequency goes higher, the switching loss goes higher, which makes the efficiency decrease as seen in Figure 2.14. The switching frequency reaching the critically frequency at around 100 kHz presents the best case.
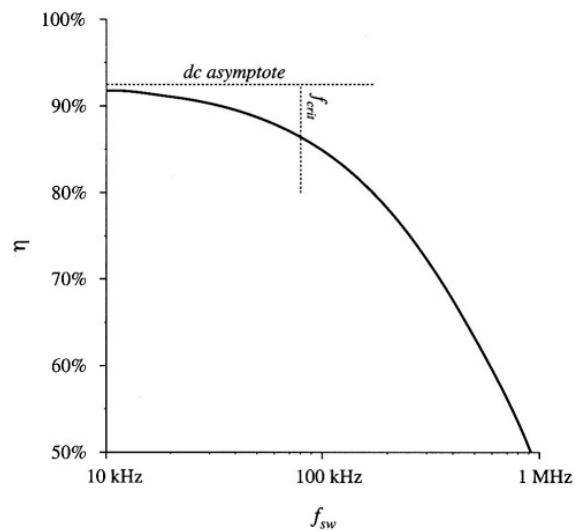
Figure 2.14 Efficiency vs switching frequency [17]

34

3.0   CONVERTER TOPOLOGIES FOR HIGH POWER APPLICATION

The three basic converters are DC-DC, DC-AC, and AC-AC. This section will briefly introduce the converter topologies and power losses dissipated by the transistors with the circuit models created via Matlab/Simulink or PSCAD and applied to the prototype that was used to measure the transistor power loss. In this chapter, the system models will be presented, and several simulations from Matlab/Simulink or PSCAD will carry out to integrate the study of the converters. The simulation results are used to investigate the power losses, efficiency, and further analysis the cost effect of the Si IGBT and SiC MOSFET devices of the system.

A high-voltage direct current (HVDC) electric power transmission system uses direct current to transmit electric power over transmission lines or submarine cables. HVDC systems have high-power capability, high stability performance, and flexible control. Direct current at low voltages could not be transmitted for long distances because of conduction losses. Low reliability, and high requirements for operation are the disadvantages of HVDC. Due to the constraints of HVDC systems, the conductivity development of wide band gap semiconductors is widely researched based on the high blocking voltage. The basic HVDC system is the conversion of electrical current from AC to DC rectifier at the transmitting end, and from DC to AC inverter at the receiving end. Figure 3.1 represents the HVDC transmission link model using 12-pulse thyristor converter via Matlab/Simulink.
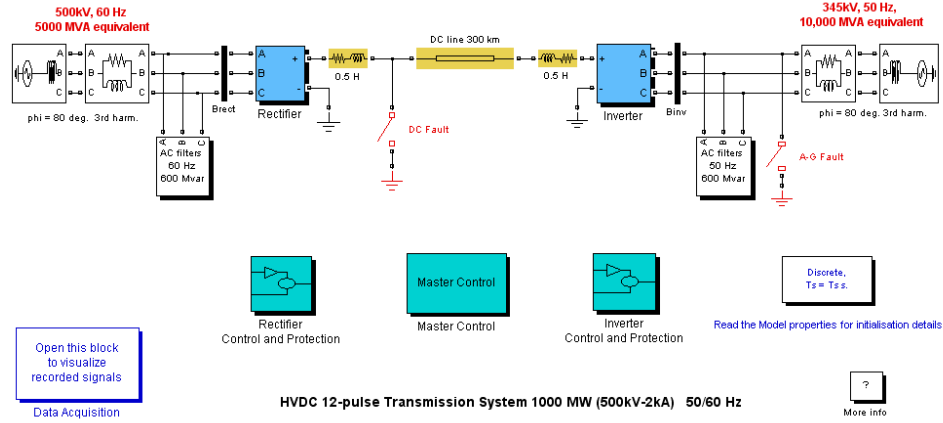
Figure 3.1 A 12-pulse converter HVDC system from Matlab Simulink (power_hvdc12pulse)

3.1 DC-DC CONVERTER TOPOLOGIES

A DC-DC converter is an electrical circuit to convert a source voltage to a different voltage level. The DC-DC converter is equivalent to a transformer since a source voltage isolates the output voltage. The regulation of the average output voltage in a DC-DC converter is a function of the on-time duty cycle. Notice that the on-time of the switch is defined as the time period that the switch is on; the duty cycle ratio is defined as the duration that the switch is active divided by the period of time as represented in Equation (14).

$$D = \frac{t_{on}}{T} \tag{14}$$

The output voltage control depends on the duty ratio D based on the type of DC-DC converters. The next section will introduce two basic DC-DC converters: boost converter and push-pull converter. It will be used and applied to the physical circuit to measure the power losses due to the specific application.

36
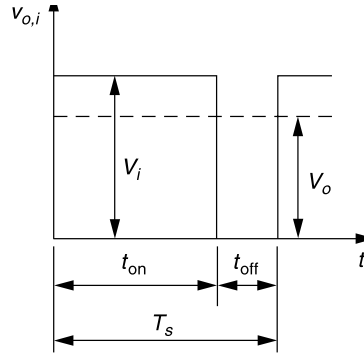
Figure 3.2 DC-DC converter voltage waveforms [44]

Pulse width modulation (PWM) is the most widely used method of controlling the output voltage. PWM switching involves comparing the level of a voltage control to the level of a repetitive waveform. [1] PWM uses a rectangular pulse wave to provide the gate voltage fed to turn the switch on and off. [5, 17]
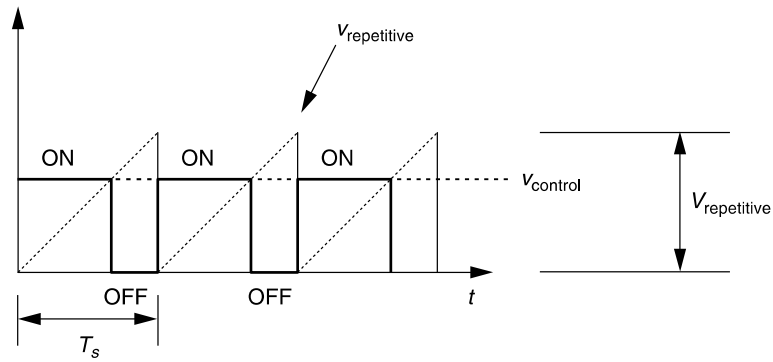
Figure 3.3 Pulse width modulation concept [16]

3.1.1 Boost (Step-Up) Converter

In a boost converter, the output voltage is greater than the input voltage. Therefore, it is called a step-up converter. The basic realization circuit is shown in Figure 3.4.
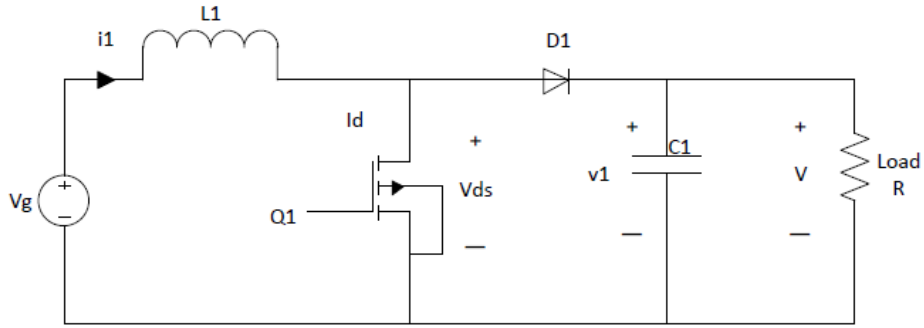
Figure 3.4 Basic boost converter circuit

When the switch is on (occurs from $0<t<DT_s$), the transistor is conducting, and the diode is reverse-biased, thus isolating the output stage as seen in Figure 3.5. The input voltage source supplies energy to the inductor.
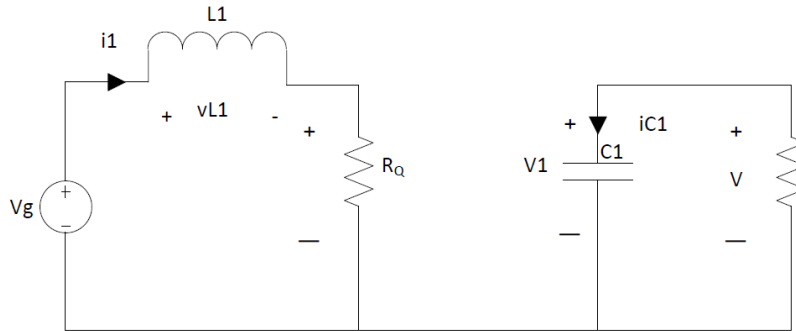
Figure 3.5 Boost converter during transistor turning on

When the switch is off, the output stage receives energy from the inductor as well as the input source. Applying the small-ripple approximation to the inductor for charging balance, the output voltage will reach a steady state, and so will the inductor current. The total volt-second balance is applied to the inductor and capacitor charge balance to find out the steady state output voltage. The voltage conversion ratio M(D) is the ratio of the output to the input voltage of a boost converter as 1/(1-D). Since D is between 0 and 1, and the output voltage is always greater than the input voltage.

38
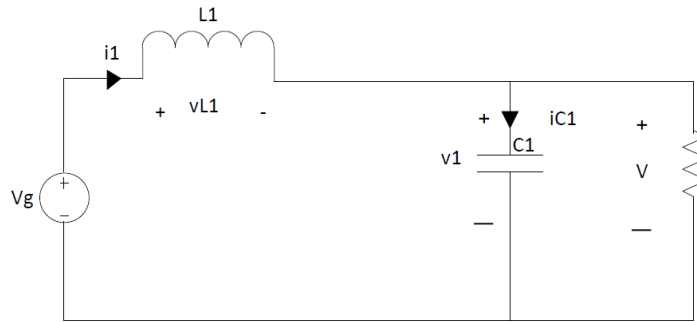
Figure 3.6 Boost converter transistor turning on, diode turning on

3.1.1.1 Boost Converter Power Losses Analysis via PSCAD

The following PSCAD experiment was to study the power losses in a boost converter. From the boost converter experiment, the power dissipated from the transistor, diode, inductor, and capacitor was obtained. Besides the physical operation of the converter, it helps to reflect on the energy transfer between the inductor and capacitor. The voltage source supplied 132.9 kilovolts. The gate driver provides $5V_{div}$ pulse width modulation in the switching operation with 1 kHz switching frequency and 50% duty cycle to both transistor modules. The diode on-resistance was set at 10 mΩ; off resistance to 1 MΩ, both the same as the transistor.

39
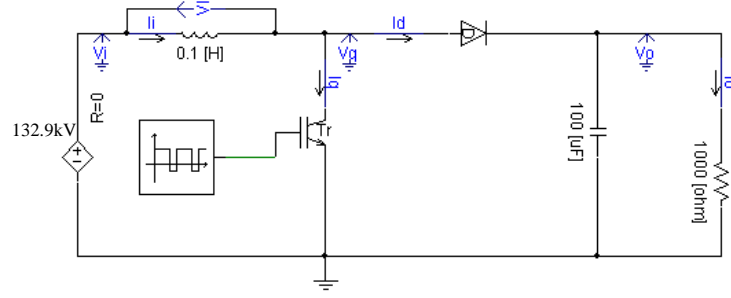
Figure 3.7 Boost converter Circuit simulation circuit via PSCAD

The input power, Pi, is equal to the input voltage times input current as shown in equation (15). Output power is output voltage multiply by output current as present in equation (16). V_g represent as the voltage across the transistor, and I_g as the current flow through the transistor, P_g as the power dissipates through it as present in equation (17). V_d represent as the voltage across the diode, which is the voltage between transistor voltage and output voltage and I_d as the current flow through the diode, P_d as the power dissipates through it as present in equation (18). Theoretically, the copper loss represents the power loss dissipates by the inductor as shown in equation (19). The capacitor loss represents the voltage and current through a capacitor; notice that the voltage across the capacitor is the same as the output voltage because the load is in parallel with the capacitor.

$$P_i = V_i * I_i \tag{15}$$
$$P_o = V_o * I_o \tag{16}$$
$$P_g = V_g * I_g \tag{17}$$
$$P_d = V_d * I_d = (V_g - V_o) * I_d \tag{18}$$
$$P_{copper} = V_L * I_L \tag{19}$$
$$P_c = V_c * I_c = V_o * I_c \tag{20}$$

40

The power loss dissipated from a boost converter represents as the power difference between input and output power (assume P_1) as presented in equation (21). Assume P_2 is the summation of diode power loss, copper loss, capacitor loss, and the transistor loss as presented in equation (22). Finally, P_{error} represents the other power losses which are expected to be zero as shown in equation (23). All the power losses were recorded in Figure 3.8 . The plots of P_1 and P_2 overlapped each other in Figure 3.8(g), indicating that the power loss dissipated from the boost converter is the power loss dissipated by the inductor, transistor, capacitor, and diode that illustrated the converter application due to the results shown in the experiment. It should be noted that P_{error} is about 0.0012 µW which is small and close to zero and could be neglected as shown in Figure 3.8(h).

$$P_1 = P_i - P_o \qquad (21)$$

$$P_2 = P_d + P_g + P_{copper} + P_c \qquad (22)$$

$$P_{error} = P_1 - P_2 \qquad (23)$$
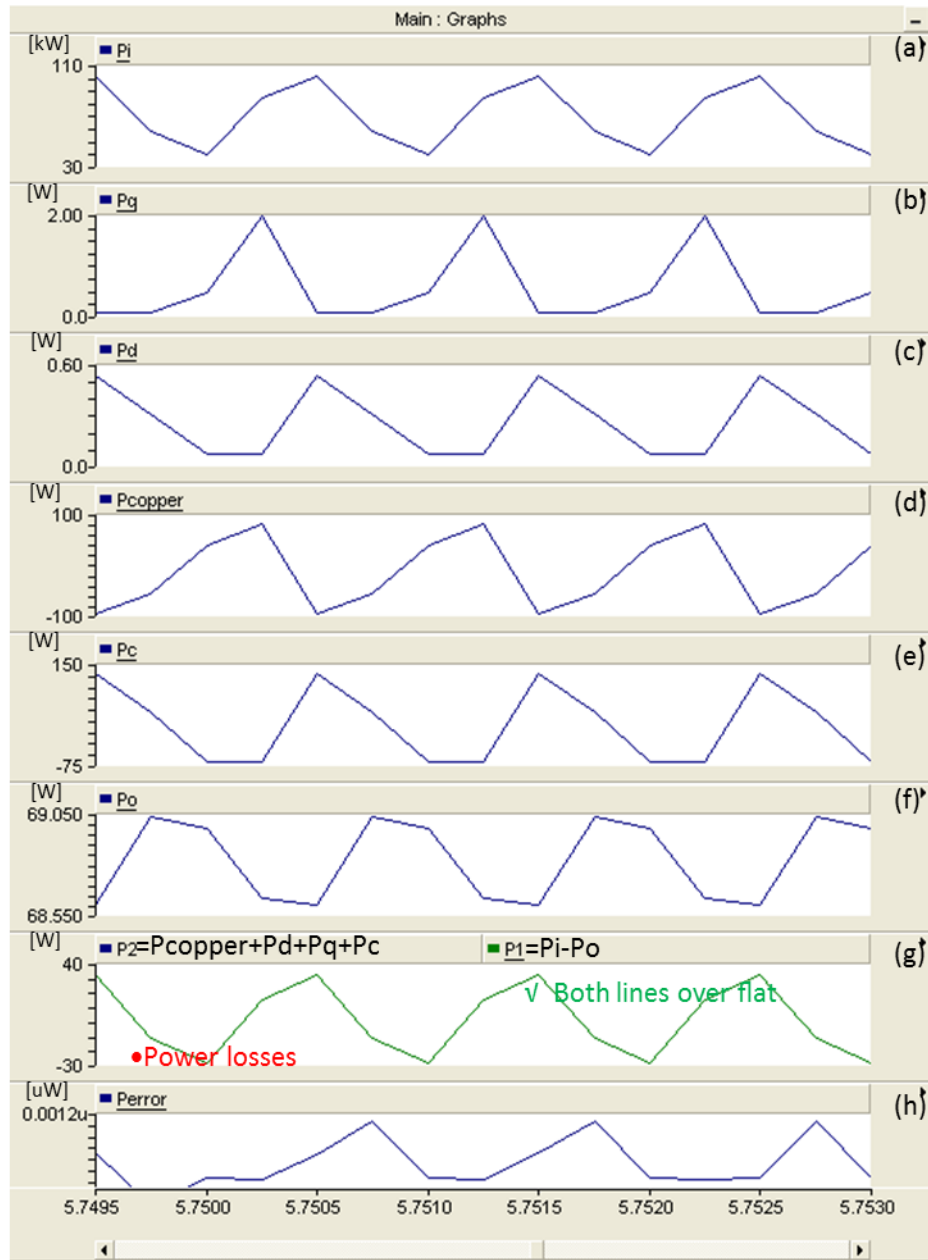
Figure 3.8 List of all power losses of the boost converter loss experiment (the boost converter with

Vs=132.9kV, L=0.1H, C=100μF, R=1kΩ)

Figure 3.9 is the plot of P_1, which is the average power dissipated during one period of time, if the area is zero, it means the assumption is correct. By calculating the average P_2 is about 0.57 W, the error P_{error} is close to zero. As a result, the assumption is proved.
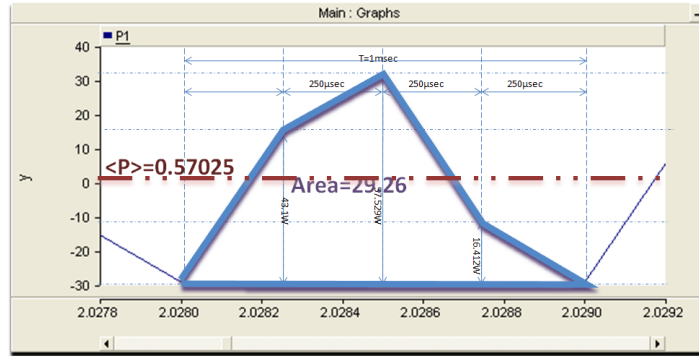
Figure 3.9 Average P₁

Section 2.3 introduces the transistor power loss which can be demonstrated as equation (17). The conduction loss is due to the current pass through the on-resistance as shown in equation (24).

$$P_{g2} = I_g{}^2 * R_{on} \qquad (24)$$

3.1.1.2 Comparative PSCAD and Matlab/Simulink Boost Converter Models of Power Losses

The boost converter of this experiment was designed to operate in the continuous conduction mode. The boost converter is a good test case since all losses— such as copper loss, diode loss, inductor loss, and capacitor loss— can easily be accounted for. When comparing the losses in the SiC MOSFET and Si IGBT, the copper, diode, inductor, and capacitor losses would be constant from trial to trial. The specific semiconductor in the circuit causes the difference between the overall losses.
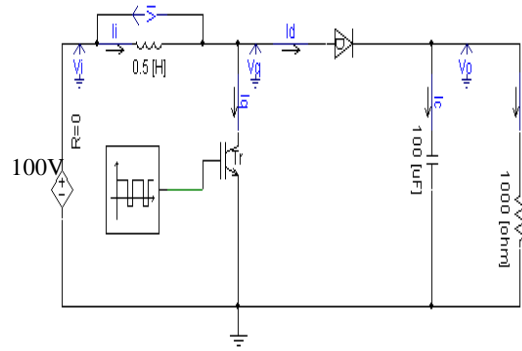
Figure 3.10 PSCAD Model of Boost Converter
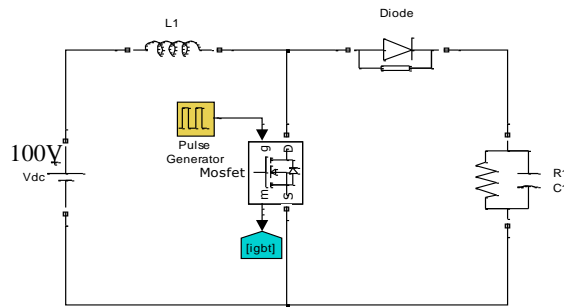
Figure 3.11 Matlab/Simulink model of Boost converter

The circuit simulation results, specifically the gate current and gate voltage of the SiC module operating with a 20 kHz switching frequency and 50% duty cycle into a 1kΩ resistive load bank are shown in Figure 3.12. Other measurements such as the inductor voltage and current, diode current, output voltage and current were also analyzed by both simulation programs. Both simulation platforms present the same results, except for the capacitor current which is caused by the charging or discharging of the capacitor. The PSCAD simulation result shows transient of the waveforms, which is not show in the Simulink results.

In comparing the power losses of the transistors in the two systems, the SiC MOSFET circuit showed superior performance with its lower power loss, higher efficiency and smaller size. The results demonstrate the potential applications of SiC technology in HVDC applications.
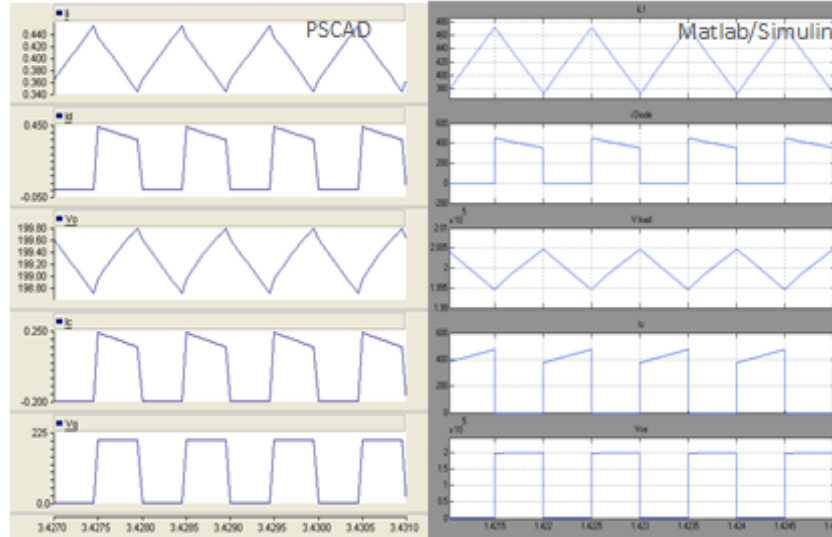
Figure 3.12 Boost converter simulation result of SiC MOSFET characteristic

3.1.2 Push-pull Converter

A push-pull converter is a DC-DC converter where a transformer is used to isolate and amplify controls the voltage source. The advantage of a push-pull converter is its ability to scale up the voltage for high power applications. The push-pull converter design allows one to perform a fair comparison between both devices, as Q1 and Q2 in Figure 3.13.
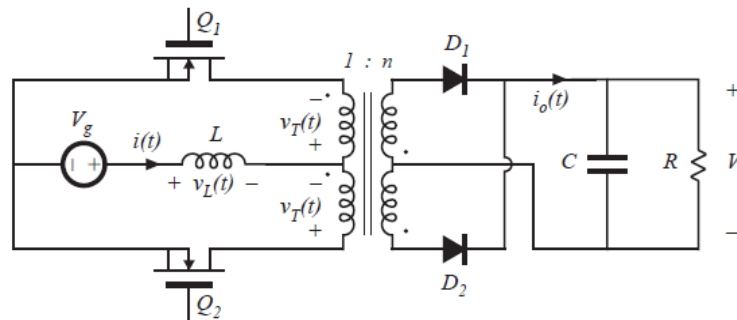
Figure 3.13 Push-pull boost-derived converter

The purpose of this study was to measure the switching losses of a silicon carbide power MOSFET device compared with a conventional Si IGBT device with similar power rating. The switching frequency is from 10k Hz to 20k Hz. The initial circuit shared the same voltage source with independent resistive load as seen in Figure 3.14. The resistive loads have the same resistance for fair comparison.
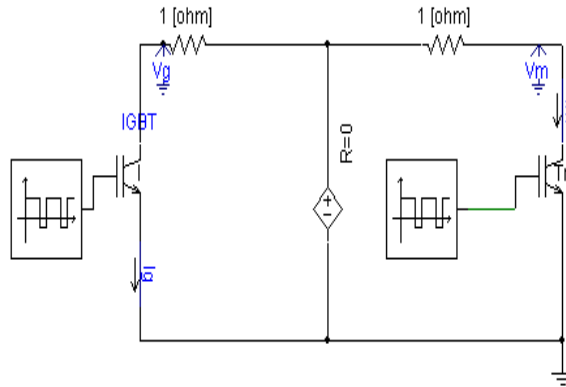
Figure 3.14 Device Circuit of IGBT and SiC MOSFET

The circuit with a 20 kHz transformer was added so that the two transistors shared the same load. The reason to use this circuit, as shown in Figure 3.15, is that the inductance of the transformer is essential to have some 'off' current flow in the Schottky diode in parallel with the FET of the Cree device.

Figure 3.15 Push-Pull design circuit for measuring the transistor loss

3.1.2.1 Comparative PSCAD and Matlab/Simulink Simulation Models of Power Losses for SiC MOSFET and Si IGBT

The objective of this research was to investigate the power losses of silicon carbide MOSFET and silicon IGBT via PSCAD and MATLAB/Simulink programs. The simplified one-line diagram of the design circuit is shown in Figure 3.17 and Figure 3.18. A push-pull converter is the acronym for the circuit. The advantage of a push-pull converter is its ability to scale voltages up to higher levels. This circuit was able to compare the power losses between SiC MOSFET and Si IGBT under the same voltage supply and same load impedance. Figure 3.17 represents the designed circuit from PSCAD and Figure 3.19 shows that from Simulink, the parameters of the power supply, transformer ratio, and load resistance were set up the same. The extra resistances from Simulink were added to simulate line resistances. The transistor parameters were set up to match the commercial SiC MOSFET and Si IGBT from data sheets.

Figure 3.16 shows the simulation results from PSCAD where both devices showed the same voltage and current waveforms. As the semiconductors present as pure resistances to the

PSCAD simulation package, when the on-resistances are the same for both transistors, the voltage and current will be the same.
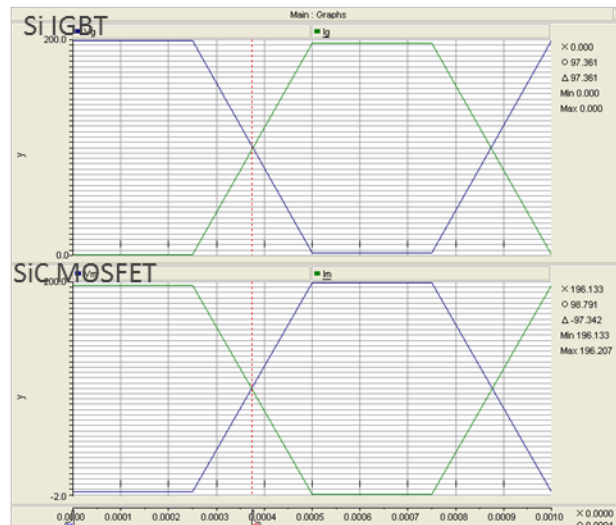
Figure 3.16 PSCAD simulation result
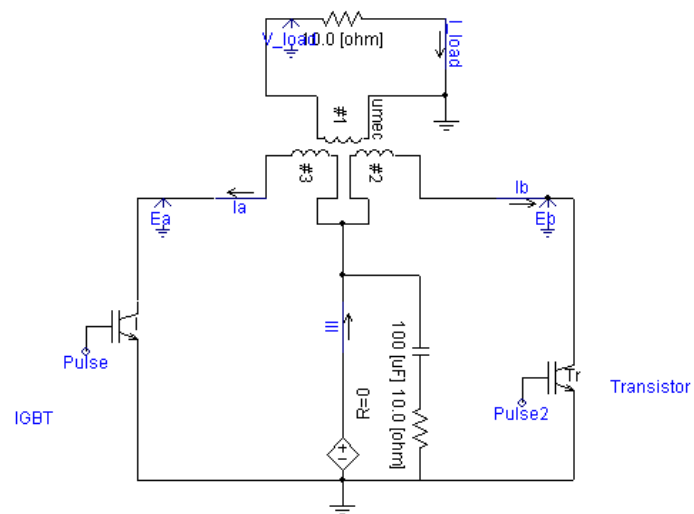
Figure 3.17 Designed push-pull circuit via PSCAD

The following model was designed to simulate the parameters from Si IGBT and SiC MOSFET from Simulink. The two resistances R2 and R4 were used prior to installation of the transformer. R5 and R6 had a small resistance to simulate line resistances. When the transformer was inserted instead of the resistors R2 and R4, the semiconductor devices had excessive currents. When the transformer was inserted into the simulation, excessive currents were recorded through the semiconductor devices. To mitigate this, extra resistances were added, preventing the back flow of current. The transistor parameters for both simulation models were obtained from the commercial SiC MOSFET and Si IGBT data sheets.
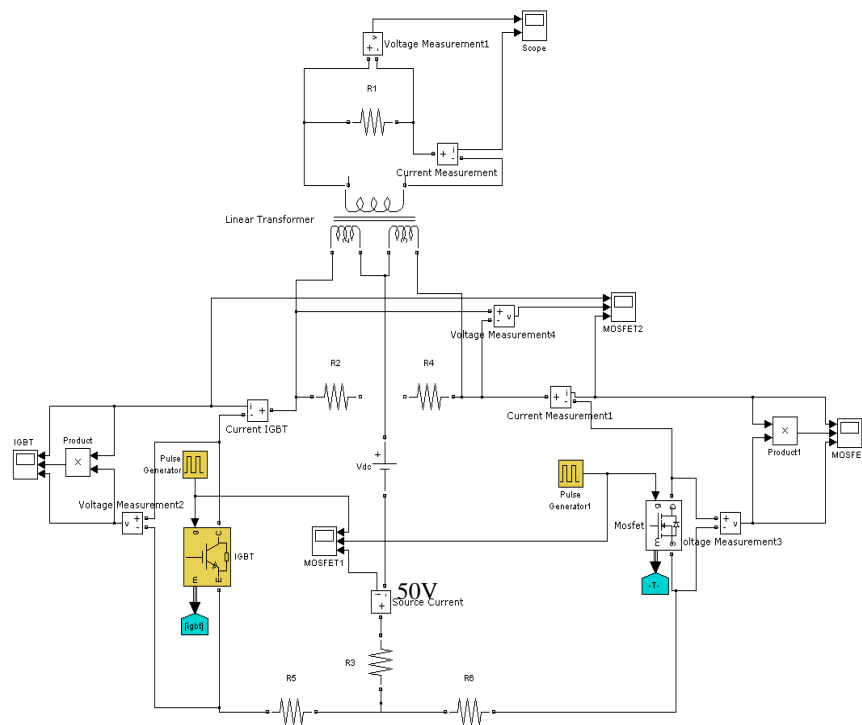
Figure 3.18 Designed circuit from push-pull converter via Simulink

Both models exhibited large voltage spikes when the current was turned off. The intrinsic inductance and capacitance lead to voltage spikes and ringing during the turn-on and turn-off

49

periods. This should be prevented by R-C snubber networks. The IGBT also had current decay time constants. Some investigation is in order on the snubber circuits and models for the IGBT and MOSFET. For example, the HVDC simulation in Matlab has IGBT's in a voltage source converter. This simulation does not have any "current decay" parameters. The voltage spikes usually cause electromagnetic interference problems which may destroy devices during the physical tests. The voltage spikes present in charge and discharge in Simulink that are not shown in PSCAD. The Simulink plot shows the switching loss of the SiC module is less than Si module. This means the SiC module has better performance for high switching frequency operation.
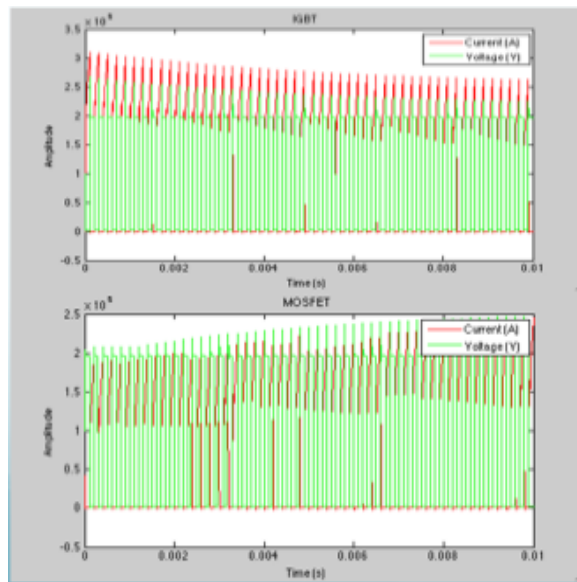
Figure 3.19 Voltage and current waveforms observe via Simulink (Top-Si IGBT; Bottom- SiC MOSFET)
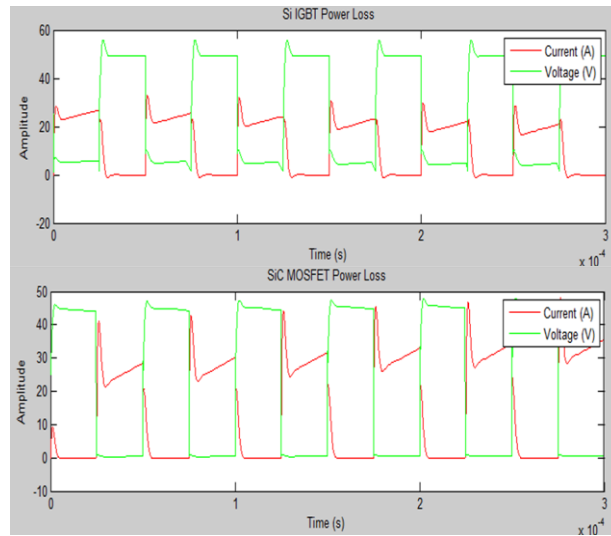
Figure 3.20 closer look of Fig3.18

3.1.2.2 Power losses calculation via Matlab

The "To workspace" blocks (Figure 3.21) allow a signal data interface from Simulink to the Matlab workspace. After sending the signal array to Matlab, one will be able to view and manage the contents of the workspace in Matlab.
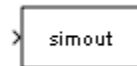
Figure 3.21 Simout block from Matlab/Simulink

For the push-pull converter that is simulated in Section 3.1.2, the voltage and current of MOSFET were interface into Matlab as seen in Figure 3.22.

51
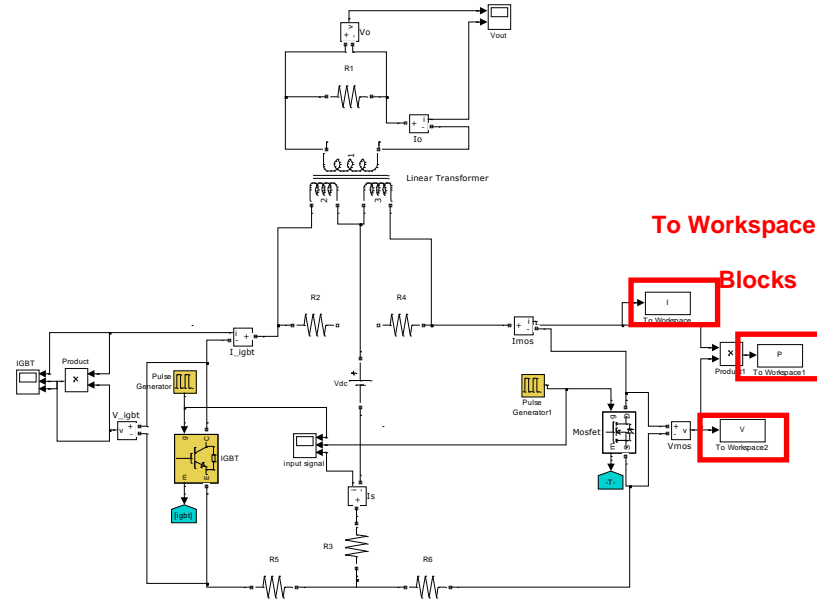
Figure 3.22 The block to interface Simulink to Matlab for calculating power losses

The signal array enables Matlab to calculate the switching and conduction loss independently by using its script language. As seen in Figure 3.23, the drain-to-source voltage (green line) and drain current (red line) of the power MOSFET are plotted. The switching losses are the losses dissipated during the switch turn-on and turn-off period, which equals the area under the volt-amp product curve. The conduction loss is the loss which occurs during conduction. The conduction loss can be calculated by forward volts-amps. A set of equations describes the behavior of power losses in Appendix A that were used to calculate the switching loss of both transistors.
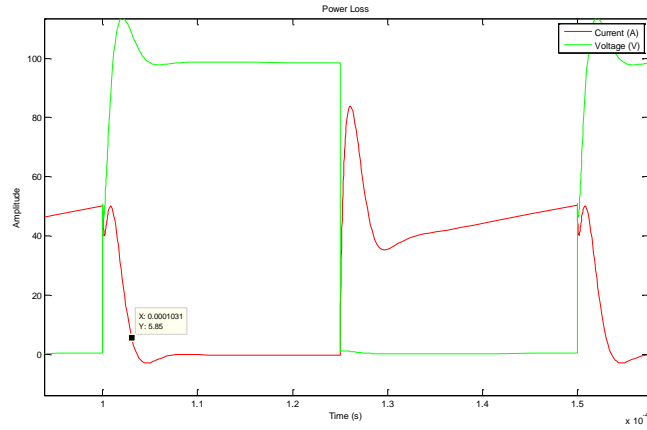
Figure 3.23 Voltage and current plotted via Matlab

The power dissipated through both transistors is tabulated in Table 3-1. The intrinsic resistance of different materials varies [1,7, 14]. The on-resistance of the silicon carbide material is much smaller than that of silicon. The conduction loss is caused by the power dissipated through the intrinsic resistance of the transistor.

Table 3-1 Matlab calculation measurements data

	Turn-on Time	Turn-off Time	Switching Loss	Conduction Loss	Total Loss
SiC MOSFET	0.18μsec	2.228 μsec	1.787mW	1.1239W	1.125W
Si IGBT	0.27 μsec	2.693μsec	2.13mW	2.0518W	2.0539W

The results show that the switching loss dissipated by the SiC MOSFET is about 19.19% less than by the Si IGBT. The conduction losses had the biggest difference between both devices. In order to reduce the conduction loss, the on-resistance must be minimized [26], which requires more silicon resulting in cost increases. Therefore, there is a trade-off between the conduction loss and the silicon cost. Besides, the result also presents that the switching turn-on and turn-off

53

time of the SiC MOSFET devices are both smaller than the Si IGBT devices. In addition, the turn-on and turn-off switching time of the SiC MOSFET are both shorter than to the Si IGBT. The results show that SiC is a better material for fast switching than Si. In conclusion, the overall results show that the SiC MOSFET is faster switching and less losses than the Si IGBT which implies that the SiC MOSFET is a better device than the Si IGBT.

3.2   AC-DC RECTIFIER

The AC-DC rectifier is used to convert AC sources to DC loads, while minimizing resistive losses. The introduction of the half-wave rectifier is presented in the following.

The half-wave rectifier will be introduced in this section. The half-wave rectifier only follows the input signal during half of the cycle. Unlike a regular half-wave rectifier, the inverting rectifier follows the signal during the negative half of the cycle. The switching device used in this experiment is a thyristor. The thyristor operates similar to a diode, in that it only operates in one-direction, and follows the input signal, unlike the diode; the thyristor has to receive a signal also, which happens at a specific time after the zero crossing. This in turn lowers the average output voltage. If this signal occurred at the zero crossing however, then the thyristor would perform the same as a diode.

The control circuit was designed to control the chip and give an output phase control proportional to the input. A low and a high side driver are needed to send the signals to the thyristor. The zero crossing detector strategy was designed to detect the transition of a signal waveform from positive and negative.
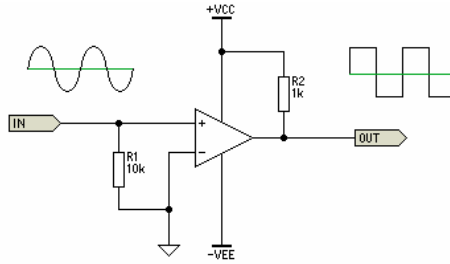
Figure 3.24 Simple zero crossing detector design for explaining transition the signal turning positive and negative

The simple zero crossing detector produces an output state change whenever the input is connected to ground. The zero crossing detector is based on a 741 op amp with a 10 kohm resistor at the input terminal, as shown in Figure 3.24. The driver will send the pulse signal to the output and turn the specified thyristor on.

The simulation of the inverting half-wave rectifier was constructed in the Matlab/Simulink design program. The requirements consisted of multiple parts: the implementation of a first-order inductive filter with $\alpha=0$, a second-order filter with $\alpha=0$, then repeated with the previous 2 filters with $\alpha=30°$, and lastly all four previous simulations with a 100mH AC-side inductance.

The first part was a simulation of the rectifier when $\alpha=0$ with a first-order inductive filter only. With $\alpha=0$, the thyristor control has the same behavior as a standard diode. The circuit is displayed in Figure 3.25. To maintain a ripple of less than 10% of the series inductor, it required a value of approximately 1H. The ripple is shown in Figure 3.26, as well as the other parameters of Vs, Is, Vd, and Io.
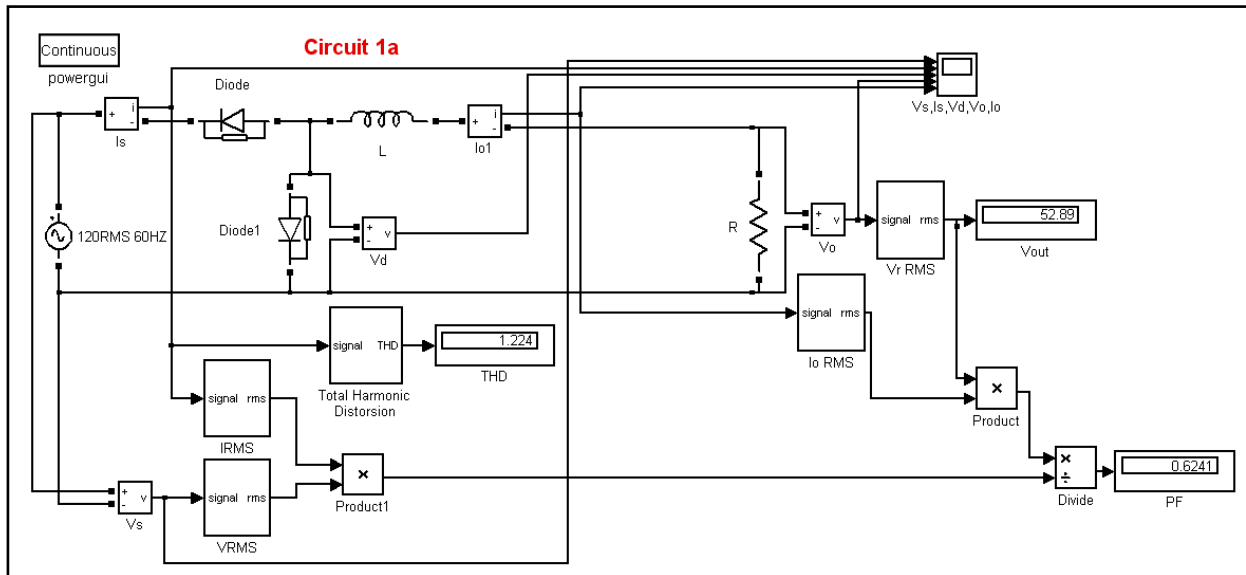
Figure 3.25 Half-wave rectifier inverter circuit of Matlab/Simulink
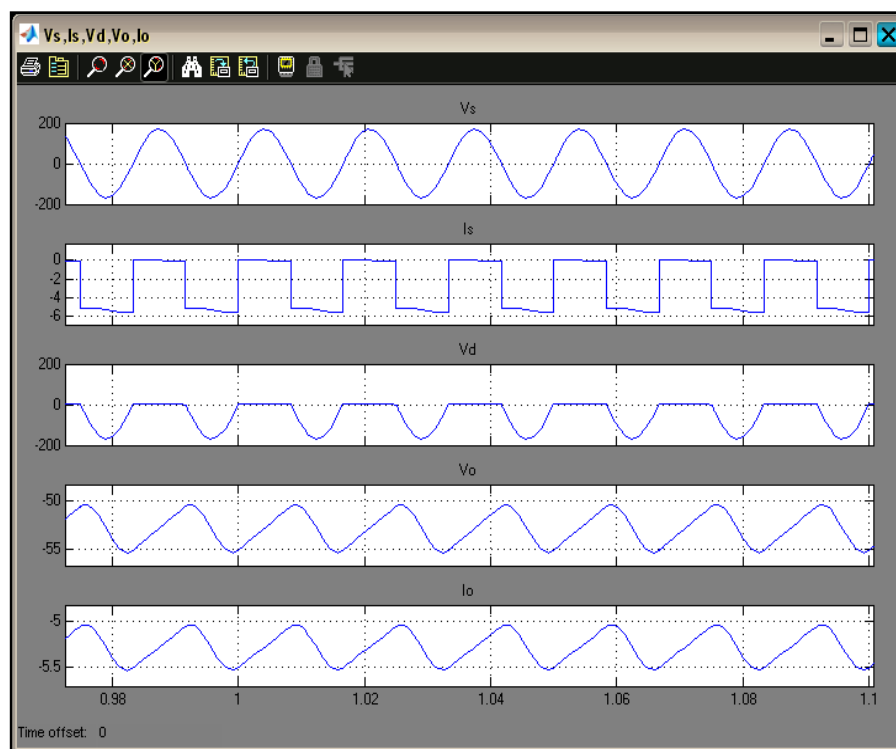
Figure 3.26 Output voltage and current waveforms ripple

One Henry is not a very realistic value to use for an inductor, so the second circuit looks to address this situation. In the second circuit, a capacitor is added to alleviate some of the demands required of the large series inductor used in circuit 1. Using a 100 mF capacitor reduced the size of the inductor by a factor of 90% to 100 mH. It also increased the output voltage to 89 Volts RMS from 53 Volts. With these performance increases, the power factor increases as well as the total harmonic distortion decreasing. Figure 3.27 shows the output of the second order filter.
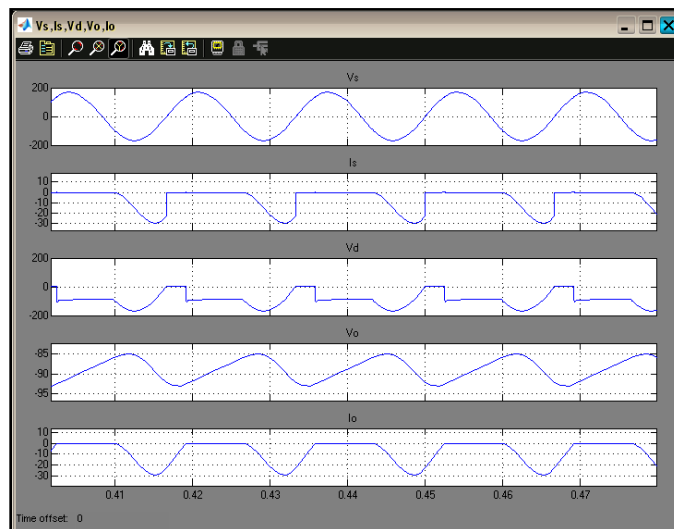
Figure 3.27 Output waveforms present the second order filter

Next, the thyristor control circuit has the firing angle delay introduced to 30°. This delay will force the thyristor to activate later than would a diode, but in turns of the thyristor will not turn off when a diode would either. This enables the circuit to be used in 2 quadrants, with the potential to behave as an inverter when $\alpha > 90°$. The thyristor control can be seen in Figure 3.28 and Figure 3.29 and the firing delay is evident in Vd of Figure 3.30. Comparing to the thyristor control with the firing delay of 30° to that of the firing angle of 0° in the first circuit, it shows

57

that the large delay nearly eliminates all DC voltage, as it is reduced to only 0.1 volts. The power

factor is reduced to almost zero, as well.
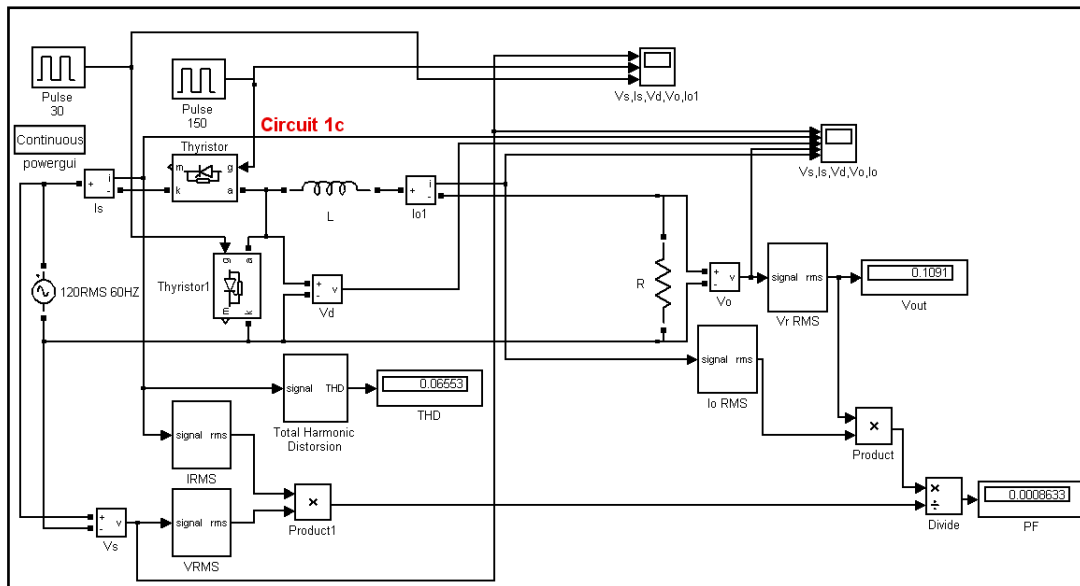
Figure 3.28 Half-wave rectifier with delay angle 30°
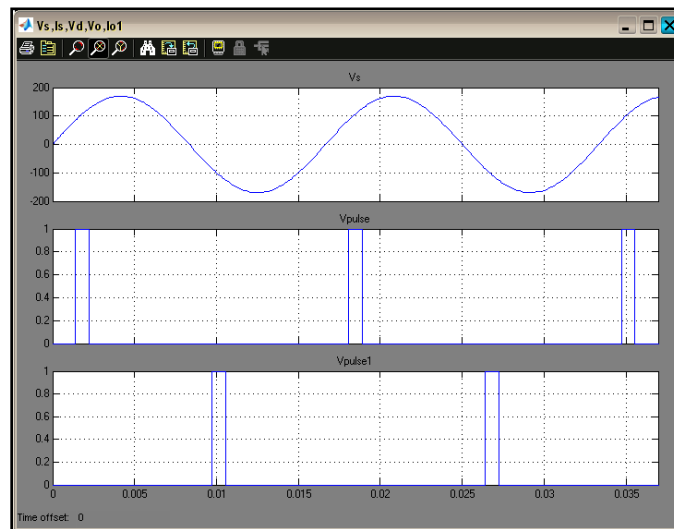
Figure 3.29 voltage and current waveform with 30-degree delay angle
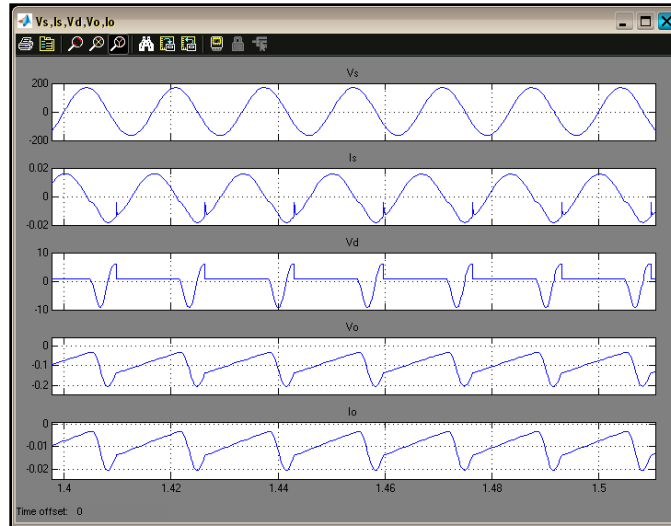
Figure 3.30 second-order voltage and current waveform with 30-degree delay angle

The basic idea of constructing the circuit for the rectifier was simple in concept for the basic power system. The capacitor, two thyristors, and power resistors were readily available and required little innovation to assemble in accordance with the provided circuit diagram. The inductor was created using an available core, assumed to be some ferrite core in which there may or may not have been an air gap. We measured the physical dimensions of the core and tried to over compensate the windings, figuring it could be trimmed if necessary.

From a simulation standpoint, the actual results of this project were closely matches with the expected results. The rectifier circuit operating normally and inverting under the circumstances that $\alpha=0°$. Adding the filters to the circuit lowered the Total Harmonic Distortion and raised the power factor, which is desirable. Also, when $\alpha=30°$ the average voltage would be less than when $\alpha=0°$, since there will be a delay in operation. Commutation adds to this delay and causes the average output voltage to be less, and the simulations support this fact.

59

3.3   COMPARATIVE RESULT OF THE SYSTEMS, REMARKS

Matlab/Simulink was able to estimate the power losses. The disadvantage of the Simulink package is that there is no direct model for real power electronics. Advantages are that the extensive control library is able to implement any control algorithm, and the graphic tools are comprehensive and easy to use. The complexity of the block diagram increase drastically when there is more than one semiconductor. Another advantage of Simulink is that the signal flow modeling can apply in different domains. Simulink is able to interface directly to Matlab. After that, the script code is able to manage and monitor the system behavior. However, there are too many unsure losses appearing. There are no directly incorporated models for real power semiconductors. Simulink simulates the test very slowly.

PSCAD has the limitation of the semiconductor devices; as a result the analysis of transistor loss is not very clear. PSCAD performs the same result for both testing circuits (push-pull converter, and boost converter). Moreover, because it doesn't present the difference of the losses between the intrinsic capacitance, PSCAD will not able to capture the device characteristics. Only a fixed step simulation is functional.

4.0   HARDWARE DEVELOPMENT EXPERIMENT

A prototype circuit was built to compare the simulation results based on the push-pull design circuit with physical measurements. The simulation packages allow performed evaluations and provide semantic details. However, the physical measurement is able to provide the sufficient accuracy of the compiler. The research is to find out how the power losses differ between SiC MOSFET and Si IGBT, while operating at 1200V/100A. Because the power supply can only provide up to 110V in the machine laboratory, the smaller power prototype was measured to evaluate if the simulators are accurate enough for future measurements. The larger capacity supplies will need to be constructed.

4.1   SYSTEM CONFIGURATION AND INTERFACE

The prototype was set up based on the circuit of Figure 3.15, with a 50 V_{DC} power supply. The rectifier design was used to enable to turn on the gate driver, and generate the voltage by the signal generator and amplify the signal. An Oscilloscope was used to monitor the voltage across the terminals and the current flowing through the two transistor devices.   The switching frequency was chosen based on the reactance and reduces the isolation.

4.2   GATE DRIVER DESIGN

A high speed op-amp logic inverter was set up to turn the MOSFET and IGBT on and off; one driven by the function generator, and another driven by the inverter generator signal. [24, 28] As mentioned in Chapter 3.3, the op-amp was built for the inverse gate signal so that when the Si IGBT turns on, the SiC MOSFET turns off, and vice versa. The gate driver provides 5 V_{div} pulse width modulation in the switching operation with 10 kHz switching frequency and 50% duty cycle to both transistor modules. As seen in Figure 4.2, the oscilloscope capture shot from the pulse width modulation voltage provide to the gate signal for both transistors are about 5V div.
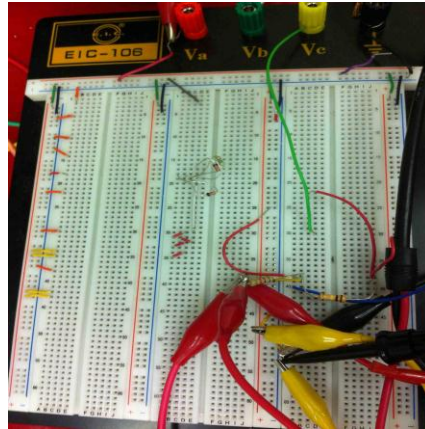
Figure 4.1 Rectifier design
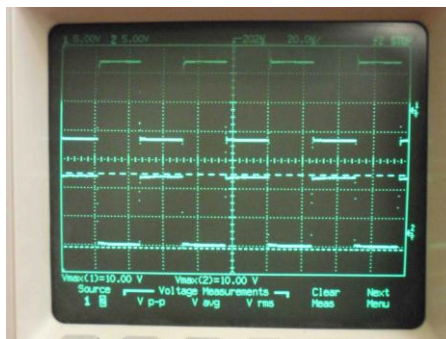
Figure 4.2 Capture of gate driver signal

62

4.3 HARDWARE CHARACTERIZATION

This section introduces the behaviors and characteristics of the devices used for the experiments.

4.3.1 SiC MOSFET- QJD1210007 (1200V/100A) [20]

Figure 4.3 SiC Power MOSFET QJD1210007 actually module

The commercial Powerex silicon carbide power MOSFET QJD1210007 module (Figure 4.3) is designed for use in high power and high frequency applications. The module is comprised of two transistors with a half-bridge configuration. At room temperature, the devices can operate up to 1200V (drain-source voltage, V_{DSS}), and 100A (drain current, I_D). The maximum power dissipation, P_D, is 880 Watts. Typical module weight is about 400g. The intrinsic parameters are listed in Table 4-1. Figure 4.4 marked out the laminated power busses, which lie across the central line of the module.
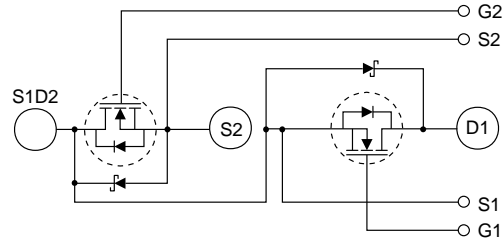
Figure 4.4 QJD1210007 circuit diagram [20]

Table 4-1 Intrinsic parameters of QJD1210007 [20]

Drain-Source On Resistance	$R_{DS(on)}$	I_D = 100A, V_{GS} = 20V	—	15	25	mΩ
		I_D = 100A, V_{GS} = 20V, T_j = 175°C	—	20	32	mΩ
Input Capacitance	C_{iss}		—	10.2	—	nF
Output Capacitance	C_{oss}	V_{GS} = 0, V_{DS} = 800V, f = 1MHz	—	1.0	—	nF
Reverse Transfer Capacitance	C_{rss}		—	0.1	—	nF
Turn-on Delay Time	$t_{d(on)}$	V_{DD} = 800V, I_D = 100A,	—	—	TBD	ns
Rise Time	t_r	V_{GS} = 0/20V,	—	—	TBD	ns
Turn-off Delay Time	$t_{d(off)}$	R_G = 10Ω,	—	—	TBD	μs
Fall Time	t_f	R_L = 856μH	—	—	TBD	ns

4.3.2 Si IGBT- CM100TF-24H (1200V/100A) [21]

Figure 4.5 Si IGBT CM100TF-24H module

64

The commercial Mitsubishi silicon IGBT CM100TF-24H module (Figure 4.5) is designed for use in switching applications with low drive power. Each module consists of six transistors with a three phase bridge configuration. At room temperature, the devices can operate up to 1200V (Collector-Emitter voltage, V_{CE}), and 100A (Emitter current, I_E). The maximum power dissipation, P_D, is 780 Watts. Typical module weight is about 830g. The intrinsic parameters are listed in Table 4-2.
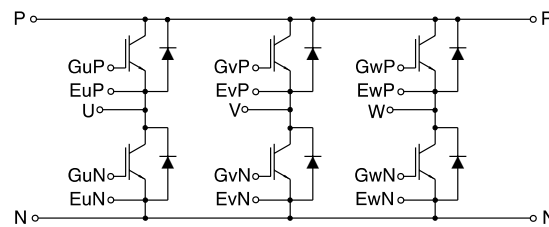
Figure 4.6 Si IGBT CM100TF-24H circuit diagram [21]

Table 4-2 Intrinsic parameters of CM100TF-24H [21]

Ratings		Symbol	CM100TF-24H				Units
Junction Temperature		T_j				−40 to 150	°C
Storage Temperature		T_{stg}				−40 to 125	°C
Collector-Emitter Voltage (G-E SHORT)		V_{CES}				1200	Volts
Gate-Emitter Voltage (C-E SHORT)		V_{GES}				±20	Volts
Collector Current ($T_C = 25°C$)		I_C				100	Amperes
Peak Collector Current		I_{CM}				200*	Amperes
Maximum Collector Dissipation ($T_C = 25°C$, $T_j \leq 150°C$)		P_c				780	Watts
Input Capacitance		C_{ies}		−	−	20	nF
Output Capacitance		C_{oes}	$V_{GE} = 0V$, $V_{CE} = 10V$	−	−	7	nF
Reverse Transfer Capacitance		C_{res}		−	−	4	nF
Resistive	Turn-on Delay Time	$t_{d(on)}$		−	−	250	ns
Load	Rise Time	t_r	VCC = 600V, IC = 100A,	−	−	350	ns
Switching	Turn-off Delay Time	$t_{d(off)}$	$V_{GE1} = V_{GE2} = 15V$, $R_G = 3.1\Omega$	−	−	300	ns
Times	Fall Time	t_f		−	−	350	ns

4.3.3   Other devices

The transformer used in the experiment is a 440 volt rms to 208 volt rms, 20 kHz, 25kVA node power transformer manufactured by the former Westinghouse Electric Corporation. The single phase transformer is configured as 208/440 volts. The primary side can be split to use in the push-pull converter test circuits.

Figure 4.7 20 kHz transformer module

The 100 Ohms resistance is also used in the experiment as shown in Figure 4.8. This resistor is able to operate up to 250W for lowest reactive components.

Figure 4.8 100 Ohms resistance

4.4   EXPERIMENT RESULTS AND DISCUSSION

The experimental system was built and verifies the design by the University of Pittsburgh, undergraduate senior design team, Mike Derrick. Figure 4.9 shows the V_{gs}, and I_{ds} behavior of the SiC MOSFET module taken from the oscilloscope, and Figure 4.10 shows the behavior for the Si IGBT module. Figure 4.9 (a) shows the oscilloscope capture, and Figure 4.9(b) shows the excel plot by the oscilloscope interface to the computer. Notice that the excel plot (Figure 4.9(b)) and the capture of Figure 4.9 (a) were taken from different time periods, and the excel plot was taken from a shorter period of time than the oscilloscope capture.
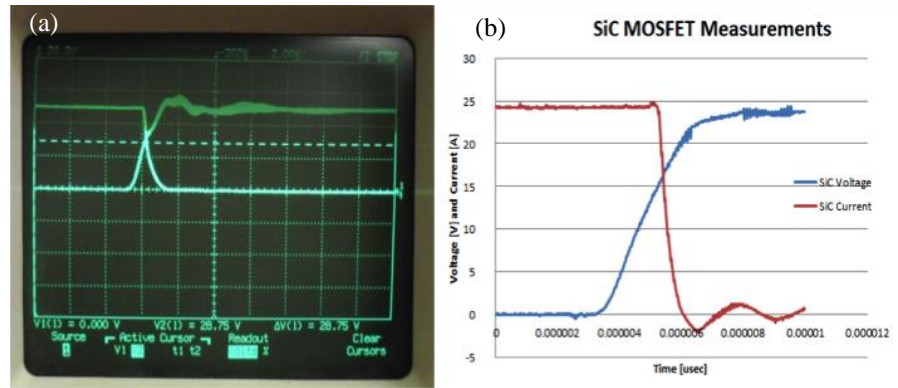
Figure 4.9 SiC MOSFET (a) Oscilloscope capture (b) Switching-off time capture from excel
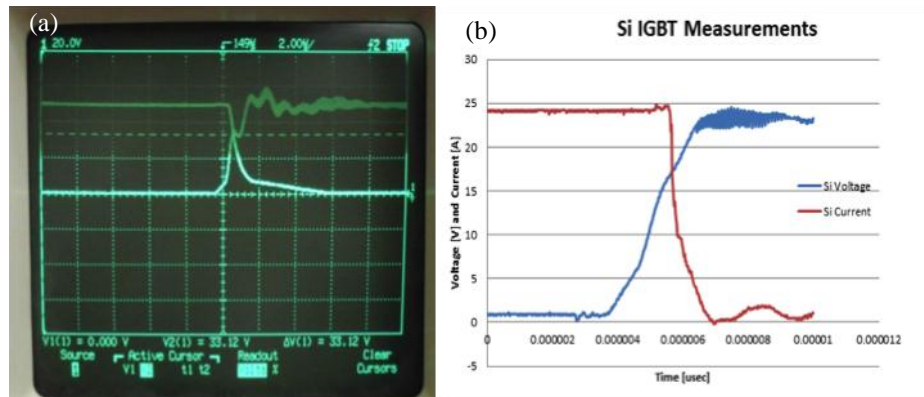
Figure 4.10 Si IGBT Oscilloscope capture (a) Oscilloscope capture (b) Switching-off time capture

from excel

The SiC MOSFET turned off faster than the Si IGBT module as shown in Figure 4.9, due to the MOSFET's intrinsic capacitance charging the device. Therefore, the forward voltage drops increased the breakdown voltage of the devices. [8] During the transistor turn off, there was a tail current in the Si IGBT due to the current, which was proportional to the stored minority charge. In contrast, since the current through SiC MOSFET module did not interrupt, the MOSFET module did not have tail current. The Si IGBT also showed more oscillation compared to the SiC MOSFET, which means the Si IGBT had less damping, and it would have less switching losses than the SiC MOSFET. The oscillation ringing indicated the switching losses decay before the

68

end of the switching period. The ringing oscillation stemmed from the mutual interactions between parasitic inductance in the circuit and terminal capacitance in the power module.

5.0   CONCLUSIONS

A circuit has been successfully designed to measure the power loss of the SiC MOSFET. With the characterization data, the SiC MOSFET model can be simulated with Matlab/Simulink, a modeling tool which takes into consideration all of the important static and dynamic characteristics of the device. The obtained MOSFET model has been verified with experimental switching waveforms and great accuracy has been achieved. The simulation results show that Matlab/Simulink provides better performance and simulation capability for computing switching losses of the semiconductor devices under investigation than PSCAD. The model was simulated with various switching frequencies and power supply voltages. Moreover, Matlab/Simulink has the ability to directly interface to Matlab and calculate the switching and conduction losses.

The goal of this project was to study the losses when both devices operate at rated voltage (1200 volts), current (100Amps), and frequency (20 kHz). The results show that the turn-on and turn-off switching time of the SiC MOSFET devices are both shorter than the Si IGBT devices. Comparing the Si IGBT device, the SiC MOSFET device has 19.19% less switching power loss. Due to the lower on-resistance of the device, the SiC MOSFET exhibits less conduction loss. Since there was no specific on-resistance for the Si IGBT device given in the data sheet, the on-resistance of the Si IGBT device was assumed to be the same as the SiC MOSFET device's on-resistance. From the simulation calculation in Matlab, the conduction loss of the Si IGBT is twice that of the SiC MOSFET. The resistivity of each material depends on the material's

electronic structure. Therefore, the resistivity of silicon must be much greater than silicon carbide to operate at the same breakdown voltage. As a result, the conduction loss of the Si IGBT is estimated to be more than twice that of the SiC MOSFET device. Based on both loss analyses, the total loss exhibited by the SiC MOSFET is much lower than the Si IGBT device.
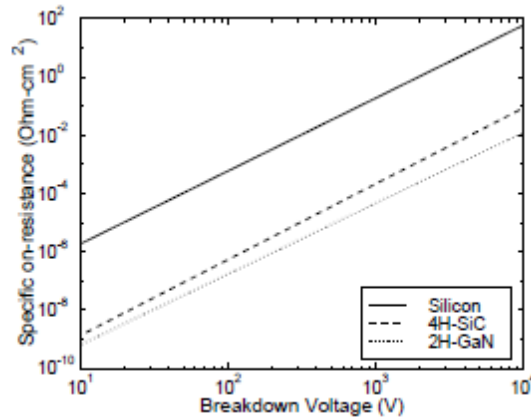
Figure 5.1 Specific on-resistance change with breakdown voltage[31]

PSCAD did not incorporate the difference between the intrinsic capacitance of different material devices. Moreover, PSCAD was not able to incorporate the difference between MOSFET and IGBT for both testing circuits. As a result, PSCAD is not a good package for power electronic simulation, when it is necessary to distinguish between the operating characteristics of different semiconductor materials.

The prototype loss analysis result also presents that the SiC MOSFET is a better material than Si IGBT for high power applications. The characterization and modeling processes are generic enough so that these methods can be applied to study new SiC devices. The SiC device has shown the desired performance compared to Si devices. The MOSFET is able to operate at higher frequency (20 kHz) with more efficient operation, better loss efficiency in soft switching applications, and longer life. In addition, the SiC MOSFET devices operating with lower

71

switching loss than the Si IGBT devices. In the final analysis, the SiC MOSFET is possible to replace the Si IGBT for HVDC applications.

For HVDC applications, the converter development requires more efficient and lower loss semiconductors. The SiC semiconductor devices have overall lower losses compare to Si-based ones. In this case, if the material price is also low, hence the SiC devices can effectively replace the Si IGBT for the HVDC systems applications.

6.0   FUTURE WORK

The higher power supply is needed to run up to 1200 volts with less interrupting signals. The current power supply in the Electric Machinery Lab at the University of Pittsburgh can generate only 110 Volts, and there is some oscillation when the voltage reaches a steady state. In addition, the external monitor control units will also help for more specific loss analysis. The SiC MOSFET is able to reduce losses. The SiC MOSFET model developed should also be used to study FACTS applications like SVC and STATCOM, as well as the use of VSC in high power transmission application, HVDC control, fault analysis with VSC technology, and dynamic response characteristics

Temperature has a strong effect on the on-resistance. Because of the majority carriers, the temperature coefficient of on-resistance is always positive. This corresponds to a conduction loss increase as the temperature goes higher. The MOSFET devices heat up very fast, so the on-resistance will not stay constant while the transistor conducts current. The model study for conduction needs to prove that the losses vary with temperature.

MATLAB SCRIPT FOR CALCULATING THE SWITCHING LOSS AND VOLTAGE

AND CURRENT PLOT

```matlab
clc
close all

figure();
plot(tout,I,'r');
hold on;
plot(tout,V,'g');
title('Power Loss');
xlabel('Time (s)');ylabel('Amplitude');
legend('Current (A)','Voltage (V)');

% for j = 1:length(I);
%     if (V(j)<I(j))
%         start = j;
%         break;
%     end
% end

% int = 0;
T = tout(end);
t = T/length(tout);
% for i = start:length(I);
%     if (V(i)>I(i))
%         int = I(i)*T+int;
%     end
% end

int1 = 0;                   %switching loss
for i = 1:length(I);
    if (V(i)>I(i))
        int1 = V(i)*I(i)*t+int1;
    end
end
```

```
result = int1/T;

%Psw=result*(ton+toff)

%%%%%%%%%%%%%%%%%%%%%%%%%%%%%%%%%%%%%%%%%%%%%%%%%%%%%%%%%%%%%%%%%%%%%%%%




int1 = 0;                    %conduction loss
for i = 1:length(I);
    if (I(i)>V(i))
        int1 = I(i)*I(i)*0.015+int1;
    end
end

result = int1;
Pcond=result*T/6
```

APPENDIX B

MATLAB SCRIPT FOR PLOTTING TOTAL POWER LOSSES

```
clc
close all

A=I.*V
max(A)
figure(2);
plot(A);
title('Power Loss');
xlabel('Time (s)');ylabel('Power [W]');
```

BIBLIOGRAPHY

[1] Baliga BJ. "Power semiconductor device figure of merit for high frequency applications" IEEE Electron Device Letters, 1989.

[2] Ruc Martin, Mitlehner H, Helbig R. SiC Devices: Physics and numerical simulation. IEEE trans Electron Devices 1994

[3] M. E. Levinshtein, S. L. Rumyantsev, and M. S. Shur, "Properties of Advanced Semiconductor Materials: GaN, AlN, InN, BN, SiC, SiGe", New York: John Wiley & Sons, Inc., 2001.

[4] Carl-Mikael Zetterling, Process Technology for Silicon Carbide Devices Docent seminar, March 21st, 2000.

[5] A. Elasser, T. P. Chow, "Silicon carbide benefits and advantages for power electronics circuits and systems," in *Proc. of the IEEE*, vol. 90, no. 6, Jun. 2002, pp. 969-986.

[6] L. D. Stevanovic, K. S. Matocha, P. A. Losee, P.A.; J. S. Glaser, J. J. Nasadoski, and S. D. Arthur, "Recent advances in silicon carbide MOSFET power devices," *Applied Power Electronics Conference and Exposition (APEC), 2010 Twenty-Fifth Annual IEEE*, vol., no., pp.401-407, 21-25 Feb. 2010 doi: 10.1109/APEC.2010.5433640.

[7] J. L. Hudgins, G. S. Simin, E. Santi, and M. A. Khan, "An assessment of wide band gap semiconductors for power devices," *Power Electronics, IEEE Transactions on*, vol.18, no.3, pp. 907- 914, May 2003.

[8] Cooper JA, Melloch MR, Woodall JM, Spitz J, Schoen KJ, Henning JP. Recent advances in SiC power devices. Materials Science Forum 1998;264(268):895±900.

[9] Y. Jang, D. L. Dillman, and M. M. Jovanovic, "Performance evaluation of siliconcarbide MOSFET in three-phase high-power-factor rectifier," in *Proc. IEEE Int'l Telecom. Energy Conf. (INTELEC) 2007*, pp. 319-326, Sept. 2007.

[10] J. Wang, L. Yang; T. Zhao; and A. Q. Huang, "Characteristics of 10 kV SiC MOSFET and PIN diode and their application prospect in high voltage high frequency DC/DC converter," *Power Electronics Specialists Conference, 2007. PESC 2007. IEEE* , vol., no., pp.72-77, 17-21 June 2007

[11] Richmond, J.; Leslie, S.; Hull, B.; Das, M.; Agarwal, A.; Palmour, J.; , "Roadmap for megawatt class power switch modules utilizing large area silicon carbide MOSFETs and JBS diodes," *Energy Conversion Congress and Exposition, 2009. ECCE 2009. IEEE* , vol., no., pp.106-111, 20-24 Sept. 2009

[12] T. Funaki, T. Kimoto, and T. Hikihara, "Evaluation of capacitance-voltage characteristics for high voltage SiC-JFET," in *IEICE Electron. Express*, vol. 4, no. 16, 2007, pp. 517-523.

[13] K. J. Schoen, J. M. Woodall, J. A, Cooper, Jr, and M. R. Melloch, "Design considerations and Experimental analysis of high-voltage SiCSchottkyBarrier Rectifiers", *IEEE Electron Device Letters*, 1998; 45(7); pp.1595-1604.

[14] J. Klein, "Application note AN-6005 Synchronous buck MOSFET loss calculation with Excel model", Fairchild Semiconductor

[15] R. W. Erickson, *Fundamentals of Power Electronics*, Kluwer Academic Publishers, Boston, 1999.

[16] N. Mohan, T.M. Undeland, and W.P. Robbins, *Power Electronics: Converters, Applications, and Design*, John Wiley & Sons, Inc., New York, 1995

[17] L. Timothy and L. Skvarenina, "The Power Electronics Handbook- Industrial electronics series", ISBN 0-8493-7336-0.

[18] Y. Xiong, S. Sun, H. Jia, P. Shea, and Z. J. Shen, "New Physical Insights on Power MOSFET Switching Losses," Power Electronics, IEEE Transactions on , vol.24, no.2, pp.525-531, Feb. 2009.

[19] D u š a n G r a o v a c , M a r c o P ü r s c h e l , Andreas Kiep, "Calculating power loss in switching MOSFETs"

[20] POWEREX, QJD1210007 SiC MOSFET Device

[21] Mitsubishi Electric, CM100TF-24H Si IGBT H-Series Module

[22] O. J. Guy, M. Lodzinski, A. Castaing, P. M. Igic, A. Perez-Tomas, M. R. Jennings, and P. A. Mawby, "Silicon carbide Schottky diodes and MOSFETs: Solutions to performance

[23] N. Mohan, T.M. Undeland, and W.P. Robbins, *Power Electronics: Converters, Applications, and Design*, John Wiley & Sons, Inc., New York, 1995 problems," *Power Electronics and Motion Control Conference, 2008. EPE-PEMC 2008. 13th*, vol.,no.,pp.2464-2471,1-3Sept.2008doi: 10.1109/EPEPEMC.2008.4635633

[24] J. Dodge, "Latest technology PT IGBTs vs. Power MOSFETs," application note APT0302 Rev. A, based on a paper presented at PCIM China 2003 Shanghai, China, April 4, 2003.

[25] S. H. Ryu, S. Krishnaswami, M. O'Loughlin, J. Richmond, A. Agarwal, J. Palmour, and A. R. Hefner, "10-kV 123-mΩ·cm2, 4H-SiC power DMOSFETs," in *IEEE Electron Device Letters*, vol. 25, no. 8, Aug. 2004, pp. 556-558.

[26] J. Qian and L. Zhao, Texas Instruments, "Circuit Design and Power Loss Analysis of a Synchronous Switching Charger with Integrated MOSFETs for Li-Ion Batteries".

[27] Fairchild semiconductor, "Effects of on resistance (Ron) to an analog switch, April 2002

[28] D. Pefrlrsis; J. Rabkowski; G. Toslstoy; H. Nee, "Experiemtntal comparison of dc-dc boost converters with SiC JFETs and SiC bipolar transistors, 2011

[29] Neudeck, P.G.; Powell, J.A.; , "Performance limiting micropipe defects in silicon carbide wafers," *Electron Device Letters, IEEE* , vol.15, no.2, pp.63-65, Feb. 1994

[30] G. Majumdar, J. Donlon, E. Motto, T. Ozeki, H. Yamamoto, M. Seto, "Present status and future prospects of SiC power devices", presentation slides by Mitsubishi Electric and Powerex

[31] K. Matocha, T.P. Chow, R.J. Hutmann, "Gallium nitride power device design tradeoffs"